J. Fluid Mech. (2015), *vol.* 780, *pp.* 503–535. © Cambridge University Press 2015
doi:10.1017/jfm.2015.468

Universality of sea wave growth and its physical roots

Vladimir E. Zakharov[1,2,4], Sergei I. Badulin[2,3,†], Paul A. Hwang[5] and Guillemette Caulliez[6]

[1]University of Arizona, Tuscon, AZ, USA

[2]Laboratory of Nonlinear Wave Processes, Novosibirsk State University, Russia

[3]P.P. Shirshov Institute of Oceanology of Russian Academy of Sciences, Moscow, Russia

[4]P.N. Lebedev Physical Institute of Russian Academy of Sciences, Russia

[5]Remote Sensing Division, Naval Research Laboratory, Washington, DC, USA

[6]Aix-Marseille Université, Université de Toulon, CNRS/INSU, IRD, MIO, UM 110, 13288, Marseille, CEDEX 09, France

(Received 24 September 2014; revised 1 June 2015; accepted 5 August 2015; first published online 7 September 2015)

Assuming resonant nonlinear wave interactions to be the dominant physical mechanism of growing wind-driven seas we propose a concise relationship between instantaneous wave steepness and time or fetch of wave development expressed in dimensionless wave periods or lengths. This asymptotic physical law derived from the first principles of the theory of weak turbulence does not contain wind speed explicitly. The validity of this law is illustrated by results of numerical simulations, *in situ* measurements of growing wind seas and wind-wave tank observations. The impact of this new view of sea-wave physics is discussed in the context of conventional approaches to wave modelling and forecasting.

Key words: air/sea interactions, surface gravity waves, wind–wave interactions

1. Introduction

Wind-driven waves are usually seen as a well-understood phenomenon of which the physics appears 'self-evident': waves are growing due to wind and dissipate due to wave breaking. This 'common-sense' understanding of sea wave physics is reflected in conventional scaling of wave growth by wind speed (e.g. Sverdrup & Munk 1947; Kitaigorodskii 1962) and in attempts to find features of wave growth universality in terms of such scaling. The non-dimensional wave height variance ε (wave energy in the wave community terminology) and the non-dimensional characteristic wave frequency, defined respectively by

$$\varepsilon = \frac{Eg^2}{U_h^4} \tag{1.1}$$

† Email address for correspondence: badulin@ioran.ru

$$\sigma = \frac{\tilde{\omega} U_h}{g}, \tag{1.2}$$

with the acceleration due to gravity g, the wind speed U_h at a reference height h or the friction velocity u^* (for a constant-flux turbulent boundary layer $u^* = (\langle U'W' \rangle)^{1/2}$), and the wave height variance $E = \langle |\eta|^2 \rangle$, are widely used in experimental and numerical studies. The characteristic wave frequency $\tilde{\omega}$ in (1.2) can be defined as the mean-over-spectrum frequency ω_m, the zero-crossing ω_z or the spectral peak frequency ω_p. Below we refer to the spectral peak frequency ω_p as the characteristic one unless otherwise stated.

Quite often results of wave studies are recapitulated in the form of power-law functions of the dimensionless time duration $\tau = tg/U_h$ or the fetch $\chi = xg/U_h^2$, as follows:

$$\varepsilon = \varepsilon_0 \tau^{p_\tau}, \quad \sigma = \sigma_0 \tau^{-q_\tau}; \quad \varepsilon = \varepsilon_0 \chi^{p_\chi}, \quad \sigma = \sigma_0 \chi^{-q_\chi}, \tag{1.3a–d}$$

that already implies, in a manner, a universality of wind wave growth. However, the coefficients ε_0, σ_0 and the exponents $p_\tau(p_\chi), q_\tau(q_\chi)$ of such parameterizations vary in a relatively wide range (e.g. $0.7 < p_\chi < 1.1$, see table 2 Badulin *et al.* 2007*a*).

We consider that the very fact of a power-like dependence of energy and representative frequency on fetch and duration is significant and requires a theoretical explanation. A number of reasons can be called upon to explain the lack of complete universality: the inadequacy of the power-law fit, the complexity of wind–wave interaction, the irrelevance of scaling by a mean wind speed with no account of the air flow stratification, gustiness etc. All these issues imply a leading effect of wind forcing rather than accounting for all the complexity of wind–sea dynamics. It leaves (intentionally or unintentionally) the inherently nonlinear dynamics of wind waves at the periphery of the discussion.

In this paper we come back to the fundamental problem of the balance between the various physical mechanisms governing wind-wave growth. In contrast to the conventional 'common-sense' understanding of this well-known natural phenomenon we develop an alternative paradigm of weakly turbulent wind-driven seas where the universality of wind-wave growth is determined, first of all, by the features of nonlinear wave–wave interactions in a random field of water waves. These features cause a strong tendency of wind-driven seas to self-similar behaviour as shown theoretically, in simulations and in analysis of experimental data (Badulin *et al.* 2002, 2005, 2007*a*, 2008; Gagnaire-Renou, Benoit & Badulin 2011). The corresponding theory predicts power-law dependence of wave energy and characteristic frequency on dimensionless duration or fetch very similar to the conventional parameterizations (1.3). The distinctiveness of the theoretical approach lies in offering an alternative scaling for describing wind-wave development that does not refer directly to wind speed.

Here we show that for duration- and fetch-limited setups wind-wave growth can be presented in a remarkably concise, but somewhat paradoxical, form that does not contain parameters of wind at all, namely

$$\mu^4 \nu = \alpha_0^3, \tag{1.4}$$

where $\alpha_0 \approx 0.7$ is a universal constant and μ, the wave steepness, is given by

$$\mu = \frac{E^{1/2} \omega_p^2}{g}. \tag{1.5}$$

The 'number of waves' ν in a spatially homogeneous wind sea (i.e. for duration-limited wave growth) is defined as follows:

$$\nu = \omega_p t. \tag{1.6}$$

For spatial (fetch-limited) wave growth the coefficient of proportionality C_f that appears in the equivalent expression $\nu = C_f|\boldsymbol{k}_p|x$ ($\boldsymbol{k}_p$ being the wavevector of the spectral peak) is close to the ratio between the phase and group velocities $C_{ph}/C_g = 2$. The universal constant α_0 in (1.4) is an analogue of the Kolmogorov–Zakharov constant of wave turbulence theory (e.g. Zakharov, Lvov & Falkovich 1992; Badulin *et al.* 2007*a*).

The relationship (1.4) can be re-written as a function of one dependent variable (e.g. μ) of another independent variable (e.g. ν); thus, it becomes a good predictive tool. An evident advantage (and surprising outcome) is that all the necessary information on wind-generated wave growth is contained in the wave data and no wind measurement is necessary for describing the wave field evolution.

Note that the dependence on wind speed can be excluded from empirical power-law fits (1.3) and a counterpart of our key result can be written in the spirit of (1.4) as follows:

$$\mu^4 \nu^r = \beta(\varepsilon_0, \sigma_0), \tag{1.7}$$

where for the duration-limited case (subscript τ)

$$r_\tau = \frac{8q_\tau - 2p_\tau}{1 - q_\tau} \tag{1.8}$$

and for the fetch-limited setup one has (subscript χ)

$$r_\chi = \frac{8q_\chi - 2p_\chi}{1 - 2q_\chi}. \tag{1.9}$$

In contrast to the theoretically based relationship (1.4) the alternative one (1.7) is not universal in two ways: the exponent r is dependent on an empirical wave growth rate and the empirical pre-exponents ε_0, σ_0 vary in a wide range as mentioned above. Thus, the physical roots of (1.4) can be discussed in terms of mechanisms that are responsible for the universal exponent r of the number of waves ν being equated to 1 in (1.7) and that makes the right-hand-side term β in (1.7) independent of wave input features. The essence of these mechanisms can be summarized in the two following issues:

(i) the dominance of nonlinear interactions in the energy balance in wind-driven seas pre-determines the essential physical links that make (1.4) a universal law without any explicit reference to wind parameters;

(ii) the ubiquity of self-similar regimes in wind-driven seas (e.g. Badulin *et al.* 2005, 2007*a*; Zakharov 2005; Gagnaire-Renou *et al.* 2011) makes the invariant (1.4) an efficient tool for physical analysis of experimental and numerical results.

In this paper, we start with a brief theoretical overview of the basic physics that leads us to the key result (1.4). More details can be found in the paper series (e.g. Badulin *et al.* 2002, 2005, 2007*a*, 2008; Pushkarev, Resio & Zakharov 2003; Zakharov 2005, 2010).

Then we present the key result of this work, the wind-free invariant (1.4), and introduce the corresponding wind-free scaling of wave growth. A number of

theoretical–empirical models of wave growth are based essentially on the physical scale of wind speed and power-law dependence of dimensionless wave height on wave period. These models and their reference exponents are well known as the Toba (1972) law of 3/2, Hasselmann *et al.* (1976) law of 5/3 and Zakharov & Zaslavsky (1983) law of 4/3. We show that the physical scales of time duration or fetch are able to replace the conventional wind speed scaling fairly well. The corresponding dependence within the new scaling gives two different exponents, namely 5/2 for fetch- and 9/4 for duration-limited cases. A key outcome of the new scaling is in eliminating any question on features of wind–wave coupling when the mean wind speed alone cannot reflect the complexity of this coupling in full.

The simple relationship (1.4) and the new wind-free scaling are verified in several examples presented in this study. All the data for the verification of the theoretical result have been obtained prior to this work. We, thus, revisit a collection of *in situ* observations (see Hwang 2006; Hwang, Garciá-Nava & Ocampo-Torres 2011, and references therein), simulations by Badulin *et al.* (2002, 2005, 2007*a*, 2008), Zakharov, Resio & Pushkarev (2012) and wind-wave tank experiments by Toba (1972), Caulliez (2013). A historical tour to the brilliant work by Sverdrup & Munk (1947) brings back the concept of significant wave height as an effective alternative to the spectral description of wind seas.

In the final section we recapitulate the various validations of the universal relationship in order to show their logical links and to outline prospects for further studies.

2. Invariant form of the self-similar solutions for growing wind seas

The core of our theoretical approach is the concept of self-similar wind-driven seas. Vladimir Zakharov was the first who reported the theoretical background and experimental illustrations of the concept (Zakharov 2002). It took three years for the paper to find a publisher (Zakharov 2005). In parallel, the ideas of the paper have been developed and supported by extensive numerical analysis (Badulin *et al.* 2002, 2005, 2007*a*,*b*, 2008; Pushkarev *et al.* 2003; Korotkevich *et al.* 2008) based on the exact simulation of spectral nonlinear transfer with the algorithm by Webb (1978, see also Tracy & Resio 1982). Independently, some features of the self-similar evolution of wind-wave spectra have been justified in Lavrenov, Resio & Zakharov (2002), Lavrenov (2003*a*) using an alternative numerical approach, the so-called Gaussian quadrature method (GQM).

Originally, the concept of self-similarity was developed for approximate solutions of the kinetic equation. Recently, exact self-similar solutions have been presented for specific functions of wind-wave external forcing (Zakharov *et al.* 2012; Pushkarev & Zakharov 2015). These input functions provide rather good fits to available empirical parameterizations and, thus, have prospects for various applications in wave modelling.

Note that self-similarity of wind seas was implied by many previous approaches, starting with the concept of significant wave height by Sverdrup & Munk (1947), developed as a similarity approach in Kitaigorodskii (1962) and Pierson & Moskowitz (1964) and then in substantial generalization of experimental and theoretical knowledge in the JONSWAP campaign (Hasselmann *et al.* 1973). The distinctiveness of the Zakharov (2005) approach that we follow in this paper is a consistent physical theory that leads to analytical results for this extremely complicated problem where such results are rare.

2.1. *The physical model of self-similar wind-driven seas*

We follow a statistical description of a random field of weakly nonlinear wind-driven waves under the effect of wind forcing and wave dissipation. The spectral density of the wave action $N(\boldsymbol{k}, \boldsymbol{x}, t)$ as a function of wavenumber $\boldsymbol{k}$, spatial coordinate $\boldsymbol{x} = (x, y)$ and time t can be described by the kinetic equation (Hasselmann 1962) as follows:

$$\frac{\partial N_{\boldsymbol{k}}}{\partial t} + \nabla_{\boldsymbol{k}} \omega_{\boldsymbol{k}} \nabla_{\boldsymbol{x}} N_{\boldsymbol{k}} = S_{nl}[N(\boldsymbol{k})] + S_{in} + S_{diss}. \tag{2.1}$$

The idea of a balance between wind input S_{in}, wave dissipation S_{diss} and wave–wave interactions S_{nl} has been circulating since long before World War II (e.g. Sverdrup & Munk 1947; Lavrenov 2003*b*). The start of the modern concept of the spectral balance of a wind-wave field is usually attributed to the paper by Gelci, Cazalé & Vassal (1957) where all the terms in (2.1) have been treated as wave-scale dependent.

The milestone papers of the early 1960s by Klauss Hasselmann (1962, 1963*a*,*b*) provided a consistent physical description of the term for four-wave resonant interactions S_{nl}. The role of these interactions in the evolution of wind-driven waves has been recognized but has not been realized in full. The basic results of the theory of weak turbulence of water waves (Zakharov & Filonenko 1966; Katz & Kontorovich 1971; Katz *et al.* 1975; Zakharov & Zaslavsky 1983; Zakharov *et al.* 1992) including those for the anisotropic Kolmogorov–Zakharov spectra (Katz & Kontorovich 1974) remained outside the chief topics studied by the wind-wave community. The efforts were focused mostly on numerical aspects of accounting for the effect of wave–wave interactions in operational and research models.

The knowledge today of the terms S_{in} and S_{diss} on the right-hand side of (2.1) is based mostly on empirical parameterizations. This represents an additional problem for wind-wave studies when correct modelling of wave evolution requires tuning to the features of a particular environment. Below we present results that do not depend on these features and do not contain any parameters of wave generation or dissipation explicitly. The physical roots of this surprising result lie in the leading role of the wave–wave interaction term S_{nl} (e.g. Hasselmann *et al.* 1973; Young & van Vledder 1993; Badulin *et al.* 2005; Zakharov & Badulin 2011): the effects of external forcing appear directly embedded in the intrinsic parameters of the nonlinear wave field.

Following the previous works (e.g. Badulin *et al.* 2005, 2007*a*; Zakharov 2005) we consider an asymptotic model describing the wind-driven seas. Assuming wave–wave interactions to be dominant compared to wind forcing and wave dissipation one can split (2.1) into two equations. In terms of the spectral energy density $E(\boldsymbol{k}, \boldsymbol{x}, t)$ the model takes the form

$$\frac{\mathrm{d}E_k}{\mathrm{d}t} = S_{nl}, \tag{2.2a}$$

$$\frac{\mathrm{d}\langle E_k \rangle}{\mathrm{d}t} = \langle S_{in} + S_{diss} \rangle. \tag{2.2b}$$

The angular brackets in (2.2) denote integration over wave scales (i.e. in wave vector space). Equation (2.2*a*) describes the effect of resonant wave–wave interactions only. Equation (2.2*b*) imposes closure conditions corresponding to the balance of the total energy: the net input (input and dissipation) is equal to the growth rate of the total wave energy. Hwang & Sletten (2008) used (2.2*b*) to address the dissipation issue of wind generated waves in field experiments.

A breakthrough can be made for deep water waves when the wave dispersion relation and the wave–wave interaction term S_{nl} are homogeneous functions of the spectral energy density $E(\boldsymbol{k}, \boldsymbol{x}, t)$ and the wave vector $\boldsymbol{k}$, i.e.

$$S_{nl}[\upsilon E(\varrho \boldsymbol{k})] = \upsilon^3 \varrho^{17/2} S_{nl}[E(\boldsymbol{k})], \tag{2.3}$$

with υ and ϱ being arbitrary positive coefficients (e.g. Zakharov 1999). This important property allows one to look for self-similar solutions as function of time (fetch) and wave frequency (wavenumber).

2.2. *Power-law dependence of the self-similar solutions*

Now we briefly outline features of self-similar solutions for the system (2.2), details being given in appendix A. Let us introduce dimensionless variables for the model (2.2) as follows (Badulin *et al.* 2005, 2007*a*; Zakharov 2005):

$$\left.\begin{aligned} \boldsymbol{\chi} = \boldsymbol{x}/l_0, \quad \tilde{\boldsymbol{k}} = \boldsymbol{k} l_0, \\ \tau = t/t_0, \quad \tilde{\omega} = \omega\sqrt{l_0/g} = \sqrt{|\tilde{\boldsymbol{k}}|}, \\ \tilde{E}(\tilde{\boldsymbol{k}}) = E(\boldsymbol{k})/l_0^4, \quad \tilde{E}(\boldsymbol{k}) = E/l_0^2. \end{aligned}\right\} \tag{2.4}$$

Note that the time and length scales t_0 and l_0 can be chosen arbitrarily in the deep water case, say, by accepting wind speed scaling (1.1), (1.2) as an option (e.g. Hwang 2006).

For the duration-limited setup one has in (2.2)

$$\frac{\mathrm{d}}{\mathrm{d}t} \to \frac{\partial}{\partial t}, \tag{2.5}$$

and the solution in the form of the so-called incomplete self-similarity can be written as

$$\tilde{E}(\tilde{\boldsymbol{k}}, \tau) = a_\tau \tau^{p_\tau + 4q_\tau} \Phi_{p_\tau}(\boldsymbol{\xi}), \tag{2.6}$$

where $\boldsymbol{\xi} = b_\tau \boldsymbol{k} t^{2q_\tau}$. Substitution of (2.6) into (2.2) leads to two constraints on parameters p_τ, q_τ and a_τ, b_τ that are of key importance for further analysis. Thus, energy growth and frequency downshift are governed by the linear relationship

$$q_\tau = \frac{2p_\tau + 1}{9}, \tag{2.7}$$

while the parameters of the solution amplitude a_τ and its width in wavenumber space b_τ obey the equation

$$a_\tau = b_\tau^{17/4}. \tag{2.8}$$

These useful relationships confirm empirical power-like laws (1.3*a*,*b*) with

$$\varepsilon_0 = a_\tau^{9/17} I_\tau, \quad \sigma_0 = a_\tau^{-2/17} J_\tau I_\tau^{-1}. \tag{2.9a,b}$$

Here I_τ, J_τ (see (A 3), (A 5) in appendix A) are integral expressions of the shape function $\Phi_{p_\tau}(\boldsymbol{\xi})$ in (2.6) that do not depend on exponent p_τ explicitly. After combining relationships (1.3*a*,*b*), (2.7), (2.9) in the form of the invariant (1.4) we observe a remarkable outcome: the result does not depend on time and initial state (i.e. on pre-exponent a_τ). Moreover, its implicit dependence on exponent p_τ is expressed

by integrals of the shape function $\Phi_{p_\tau}(\boldsymbol{\xi})$. Assuming spectral shape invariance, i.e. integrals I_τ, J_τ to be constants, we get immediately that α_0 in (1.4) is constant. This is what we call the universality of wind-driven seas.

Note that the assumption of spectral shape invariance is introduced here for the integral quantities I_τ and J_τ and is not equivalent to a point-by-point matching of the shape functions $\Phi_{p_\tau}(\boldsymbol{\xi})$ for different exponents p_τ. This assumption has been carefully checked in previous extensive numerical studies (Badulin *et al.* 2005, 2007*a*, 2008). A similar assumption has been exploited by Hasselmann *et al.* (1976, see § 2).

The same universal behaviour holds in the fetch-limited setup. Now one has

$$\frac{\mathrm{d}}{\mathrm{d}t} \to \frac{\partial \omega}{\partial k}\frac{\partial}{\partial x}, \tag{2.10}$$

and the self-similar solution is given by the expression

$$\tilde{E}(\tilde{\boldsymbol{k}}, \chi) = a_\chi \chi^{p_\chi + 4q_\chi} \Phi_{p_\chi}(\boldsymbol{\zeta}), \tag{2.11}$$

with $\boldsymbol{\zeta} = b_\chi \tilde{\boldsymbol{k}} \tilde{x}^{2q_\chi}$. Again, substitution into (2.2) gives links between exponents

$$q_\chi = \frac{2p_\chi + 1}{10} \tag{2.12}$$

and pre-exponents

$$a_\chi = b_\chi^{9/2}. \tag{2.13}$$

Similarly to the duration-limited case the pre-exponents of wave growth in (1.3*c*,*d*) are

$$\varepsilon_0 = a_\chi^{5/9} I_\chi, \quad \sigma_0 = a_\chi^{-1/9} J_\chi I_\chi^{-1}. \tag{2.14a,b}$$

It is easy to check that the invariant (1.4) keeps the same form as the one in the duration-limited case with the number of waves ν defined in terms of spatial wave period. Again, the invariant does not depend on time and initial state (i.e. on pre-exponent a_χ). The implicit dependence of the integrals I_χ and J_χ in (A 10), (A 13) on exponent p_χ is weak and the assumption of spectral shape invariance can be accepted to fix the right-hand-side value as constant α_0.

2.3. *Universal constant α_0 for duration- and fetch-limited setups*

The importance of links between parameters of self-similar solutions (2.7), (2.8), (2.12), (2.13) was first realized by Badulin *et al.* (2007*a*, see (1.9)) in the form of the so-called weakly turbulent law of wind-wave growth

$$\frac{E\omega_p^4}{g^2} = \alpha_{ss} \left(\frac{\omega_p^3 \,\mathrm{d}E/\mathrm{d}t}{g^2} \right)^{1/3}. \tag{2.15}$$

Here α_{ss} is a coefficient that depends on the exponent of wave energy growth p_τ (p_χ) only. Assuming spectral shape invariance (quasi-universality of spectral shape in the words of Badulin *et al.* 2007*a*) one obtains $\alpha_{ss} \sim p_\tau^{-1/3}$ ($\alpha_{ss} \sim p_\chi^{-1/3}$). For a given parameter $p_\tau(p_\chi)$, i.e. for a power-law growth of wave energy, the relationship (2.15) allows for the conversion of the instant wave energy and frequency into the instant wave input or vice versa (see § 5 in Badulin *et al.* 2007*a*).

In contrast to α_{ss} in (2.15), α_0 in the invariant (1.4) is constant (with the assumption of spectral shape invariance) and the invariant itself does not contain time or space

derivatives but physical quantities that we are interested in only (wave height and period). Thus, the conservation law (1.4) can be treated as an adiabatic invariant for (2.15) and for the corresponding families of self-similar solutions of the model (2.2) with $p_\tau(p_\chi)$ being formally a slowly varying parameter. The features of this adiabatic invariant are, first, independence of the parameter of adiabaticity $p_\tau(p_\chi)$ and, secondly, independence of the initial state of the system. The first one implies an arbitrary dependence of wave growth on time or fetch. The second feature looks strange amongst examples of classic mechanics when a conservative quantity, say the wave action of an oscillator, is determined by its initial energy and frequency. In fact, our special case reflects an asymptotic nature of the self-similar solutions of the kinetic equation and their inherent nonlinearity that forces the system to forget the initial state.

It is useful to specify different values of the constant α_0 in (1.4) for duration- and fetch-limited setups. The correspondence of these cases comes directly from the relationships between the partial derivative in time and the convective operator in the model (2.2), i.e.

$$\frac{\mathrm{d}}{\mathrm{d}t} \to \frac{\partial}{\partial t} \to V\frac{\partial}{\partial x}. \tag{2.16}$$

The velocity V is associated with averaging the wave energy flux over the wave-scale range, i.e.

$$\langle C_g(\boldsymbol{k})E(\boldsymbol{k})\rangle = V\langle E(\boldsymbol{k})\rangle. \tag{2.17}$$

Generally, V differs from the group velocity of the spectral peak given by

$$C_g(\omega_p) = 0.5\frac{g}{\omega_p}, \tag{2.18}$$

a quantity we are exploiting in our analysis. This case allows a simple definition of the number of waves ν in the fetch-limited case, that is

$$\nu = 2|\boldsymbol{k}_p|x, \tag{2.19}$$

which will be used below in this paper for the fetch-limited case. Furthermore, to check the law (1.4) we take the definitions (1.6) and (2.19) for duration- and fetch-limited cases respectively as follows:

$$\mu^4\nu = \alpha_{0(d)}^3 \quad \text{or} \quad \mu^4\nu = \alpha_{0(f)}^3. \tag{2.20a,b}$$

The notation α_0 without the extended subscript is used below provided this does not lead to confusion. Following Badulin *et al.* (2007*a*) and Gagnaire-Renou *et al.* (2011) one can obtain the two estimates

$$\alpha_{0(d)} = \alpha_{ss}^{(d)}p_\tau^{1/3} \approx 0.70, \tag{2.21}$$

$$\alpha_{0(f)} = \alpha_{ss}^{(f)}p_\chi^{1/3} \approx 0.62. \tag{2.22}$$

The difference in magnitude of $\alpha_{0(d)}$ and $\alpha_{0(f)}$ can be partially related to the difference in shape of the wave spectra of duration- and fetch-limited seas. This is unlikely to be the major effect if we accept spectral shape invariance. It is more natural to treat the small (about 10 %) difference as one between the characteristic velocity V and

the group velocity of the spectral peak. If we are looking for a 'perfect universality' of our law, i.e. equivalence between $\alpha_{0(f)}$ and $\alpha_{0(d)}$, we have to take into account this difference between V and $C_g(\omega_p)$ in the definition of the number of waves ν in (2.19), i.e.

$$\frac{V}{C_g(\omega_p)} = \left(\frac{\alpha_{0(f)}}{\alpha_{0(d)}}\right)^3 \approx 0.7. \tag{2.23}$$

The characteristic velocity V for wind-wave spectra appears to be approximately 30 % smaller than that of the spectral peak $C_g(\omega_p)$ which matches quite well with previous experimental results (e.g. Yefimov & Babanin 1991; Hwang & Wang 2004; Hwang 2006).

3. Physical scaling of growing wind seas and the first test of the universality of wind-wave growth

The theoretical results of the previous section look paradoxical and contradictory to a common sense understanding of wind-wave dynamics: the invariant (1.4) does not refer to any wind parameters. All the complexity of wind-wave coupling is embedded in the intrinsic wave parameters, i.e. the wave steepness μ and the dimensionless number of waves ν. Thus, the common sense notion of 'wind rules waves' should be replaced by a new one:

'waves chronicle wind development',

as a balance between the number of waves ν and their wave steepness μ (i.e. nonlinearity). This new formulation, first, implies a new physical scaling that will be introduced below. The consistency of the new formulation with previous experimental and theoretical results will be detailed in order to show the correspondence of this formulation with results inherently based on a wind speed scaling.

3.1. *Physical scaling of self-similar wave growth*

The invariant (1.4) of self-similar solutions for wind-driven seas can be written in the form of a dependence of wave height on wave period. An example of such a dependence is the famous Toba (1972) law of 3/2 (the dimensionless wave height is proportional to the power 3/2 of non-dimensional wave period). The key difference of the new dependence is in the physical scaling: the conventional scaling is based on wind speed (1.1), (1.2) while the new one implied by invariant (1.4) is wind-speed free.

Let us introduce the dimensionless wave height and period for the fetch-limited case as follows:

$$\tilde{H} = \frac{H_s}{x}, \quad \tilde{T} = T\sqrt{\frac{g}{8\pi^2 x}}, \tag{3.1a,b}$$

for fetch x, the spectral peak period T and the significant wave height $H_s = 4\sqrt{E}$. For the duration-limited case similar quantities can be introduced as

$$\tilde{H} = \frac{H_s}{gt^2}, \quad \tilde{T} = \frac{T}{2\pi t}. \tag{3.2a,b}$$

The dimensionless periods defined by (3.1), (3.2) have a simple physical meaning as they express wave lifetime in terms of the number of instantaneous temporal or spatial wave periods. For the duration-limited case (3.2) it follows that

$$\tilde{T} = \nu^{-1}, \tag{3.3}$$

and for the fetch-limited case (3.1)

$$\tilde{T} = \nu^{-1/2}. \tag{3.4}$$

Definitions (3.3), (3.4) represent a kinematic treatment of invariant (1.4): the instantaneous wave steepness is thus determined by the time (distance) of wave evolution expressed in dimensionless instantaneous wave periods.

One can propose a dynamical interpretation of (1.4). The μ^4 defined by (1.5) gives a scale for the nonlinear relaxation of a deep-water wave field (see (22), (23) in Zakharov & Badulin 2011). Thus, one can treat dimensionless time ν as a dynamical lifetime:

$$\tilde{T} = B\alpha_0 \frac{\tau_{nl}}{T}, \tag{3.5}$$

where τ_{nl}, given by

$$\tau_{nl} = (B\omega_p \mu^4)^{-1}, \tag{3.6}$$

is a characteristic time of the nonlinear relaxation of a deep-water wave field. B is a large coefficient as shown by Zakharov & Badulin (2011) ($B = 36\pi$ in the limit of a narrow angular wave spectrum, $B = 22.5\pi$ for an isotropic wave field). Thus, (1.4) states that the wave age $t\tau_{nl}^{-1}$ measured on the nonlinear relaxation scale τ_{nl} remains constant for growing wind waves. In accordance with (3.5) and estimates by Zakharov & Badulin (2011) time t does not exceed 100 relaxation times τ_{nl}.

Within the new wind-free scaling (3.2) one gets a law of 9/4 for the duration-limited setup, namely

$$\tilde{H} = 4\alpha_{0(d)}^{3/4} \tilde{T}^{9/4} \approx 3.06 \tilde{T}^{9/4}. \tag{3.7}$$

The fetch-limited dependence differs from (3.7) by a factor of 2, but, what is more significant is the exponent. It gives a 5/2 law:

$$\tilde{H} = 8\alpha_{0(f)}^{3/4} \tilde{T}^{5/2} \approx 5.59 \tilde{T}^{5/2}. \tag{3.8}$$

The difference between the exponents in (3.7) and (3.8) provides a quantitative criterion for discriminating between spatial and temporal scenarios of wave growth.

3.2. *A parametric model by Hasselmann et al. (1976) and universality of wave growth*

The exponents 9/4 and 5/2 in (3.7), (3.8) look confusing in view of their counterparts of dimensionless single-parameter dependence of wave height on period scaled by wind speed (e.g. Toba 1972; Hasselmann *et al.* 1976; Zakharov & Zaslavsky 1983). The latter set of exponents conforms with a specific ABC of wind-wave growth (see Badulin 2010). These well-known exponents of 5/3 (Hasselmann *et al.* 1976), 3/2 (Toba 1972) and 4/3 (Zakharov & Zaslavsky 1983) correspond to different reference regimes of wind–wave coupling associated with permanent fluxes of momentum, energy and wave action (Gagnaire-Renou *et al.* 2011; Badulin & Grigorieva 2012). The laws of 9/4 and 5/2 presented above do not allow one to discriminate between these reference dynamical regimes of wave growth. Instead, they describe a continuous evolution from one regime to the other in a universal way. We will show in the following analysis of the wave prediction model by Hasselmann *et al.* (1976) that these laws are fully consistent with the previous studies.

3.2.1. *Self-similarity of the spectral shape*

Hasselmann *et al.* (1976) started with the JONSWAP parameterization of a wind-wave spectrum (Hasselmann *et al.* 1973) as a function of five parameters. Then they exploited empirical links between these parameters and wind speed in order to describe the spectral evolution in terms of a set of partial differential equations.

In contrast to this parametric approach we get self-similar solutions as functions of a set of four parameters $a_\tau, b_\tau, p_\tau, q_\tau$ $(a_\chi, b_\chi, p_\chi, q_\chi)$ from the asymptotic model (2.2). Consistency of the model imposes two links between these parameters (2.7), (2.8), (2.12), (2.13). The explicit shape of the solutions (functions Φ_{p_τ} and Φ_{p_χ}) is of no importance in this case. Thus, both the approach by Hasselmann *et al.* (1976) and ours follow the concept of self-similarity in very similar ways as further discussed below.

3.2.2. *The balance between nonlinear transfer and external forcing*

A condition of permanent wind stress exerted on waves (in other words, constant wave momentum flux or constant drag coefficient) is introduced to close the balance of the wave energy in the model of Hasselmann *et al.* (1976, see (3.4)). It fixes the ratios $q_\tau/p_\tau = 3/10$ $(q_\chi/p_\chi = 3/10)$ for both duration- and fetch-limited cases. Note that only the ratio is fixed, the exponent q (or p) itself remains a free parameter.

Alternatively, the balance (2.2*b*) and its counterpart (2.15) treat the balance in terms of total fluxes of energy, momentum or wave action without any explicit reference to wind speed and features of wind–wave coupling. As a result, the growth rate $p_\tau(p_\chi)$ appears to be linked to the frequency downshift exponent $q_\tau(q_\chi)$ exclusively by the properties of homogeneity of the kinetic equation (2.3). The corresponding linear relationships (2.7), (2.12) do not follow the ratio $q_\tau/p_\tau = 3/10$ $(q_\chi/p_\chi = 3/10)$ given by the model of Hasselmann *et al.* (1976). Within our approach the dependence of spectral fluxes on time or fetch are not restricted by additional assumptions of constant wind stress or any other specific scenarios of wave input. Thus, the approach can be regarded as more general than the theoretical–empirical model by Hasselmann *et al.* (1976).

3.2.3. *Shape invariance of wave spectra*

Another parallel between the two theories can be found in the assumption of quasi-universality (as defined by Badulin *et al.* 2007*a*, and in § 2.3) or shape invariance of wave spectra (in the words of Hasselmann *et al.* 1976). The integral properties of wave spectra depend on total energy and a characteristic frequency only and can be assumed to be independent of fetch or duration because this weak 'dependence is not discernible within the scatter of the JONSWAP spectra' (see p. 203 in Hasselmann *et al.* 1976). Similarly, in our work we assume integrals of spectral shape functions I_d, I_f, J_d, J_f (A 3), (A 5), (A 10), (A 13) to be independent of wave growth rate $p_\tau(p_\chi)$ in order to get the universal invariant of wave growth (1.4). We stress that in both theories, the spectral shape invariance refers to integral quantities and does not require point-by-point proximity of spectral distributions.

3.2.4. *Special solutions by Hasselmann et al. (1976) and wave growth universality*

A remarkable feature of the Hasselmann *et al.* (1976) work is that their solutions (see § 5 therein) can be written in the form (3.7), (3.8). Following the notation of Hasselmann *et al.* (1976, (5.3)–(5.10) therein) one can obtain for duration- and

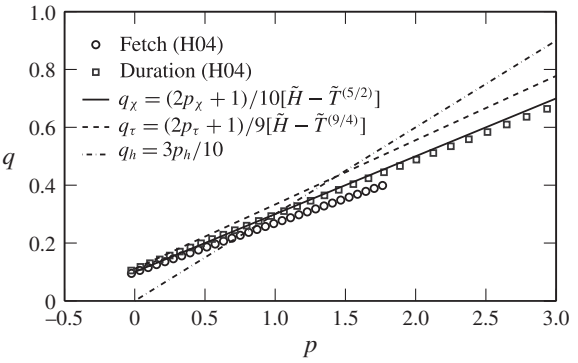

FIGURE 1. Dependence of frequency downshift exponent q on energy growth exponent p for duration- and fetch-limited setups for experimental fits by Hwang & Wang (2004) (symbols), the theory of this paper (solid and dashed lines) and the theory of Hasselmann *et al.* (1976) (dash-dotted line).

fetch-limited cases, respectively,

$$\tilde{H} = 4(2\pi)^{9/4} C^{1/2} A^{7/12} \tilde{T}^{9/4}, \tag{3.9a}$$

$$\tilde{H} = 4(8\pi^2)^{5/4} C^{1/2} A^{5/6} \tilde{T}^{5/2}. \tag{3.9b}$$

Here the parameter of spectral shape invariance can be assumed to be constant, $C = 5.1 \times 10^{-6}$ (Hasselmann *et al.* 1976). The coefficient A in (3.9*a*,*b*) depends weakly on parameters of solutions and can be assumed constant as well, i.e. $A = 16.8$ for duration- and $A = 2.84$ for fetch-limited cases (see Hasselmann *et al.* 1976, (5.7)–(5.10)). Substituting these values into (3.9*a*,*b*) one gets, respectively,

$$\tilde{H} \approx 2.93\tilde{T}^{9/4}, \tag{3.10a}$$

$$\tilde{H} \approx 5.07\tilde{T}^{5/2}. \tag{3.10b}$$

The coefficients in (3.10*a*,*b*) are quite close to those of our theory (cf. (3.7), (3.8)) and correspond to (cf. (2.21), (2.22))

$$\alpha_{0(d)} = 0.660, \quad \alpha_{0(f)} = 0.545. \tag{3.11a,b}$$

The formulae derived by Carter (1982) on the basis of the theory by Hasselmann *et al.* (1976) give slightly different estimates of the coefficients in (3.10*a*), i.e. 2.92 rather than 2.93 with $\alpha_{0(d)} = 0.658$, and in (3.10*b*) 4.99 instead of 5.07 with $\alpha_{0(f)} = 0.533$.

To end this section it is stressed that there is a deep correspondence between the theoretical–empirical approach by Hasselmann *et al.* (1976) and the theoretical one developed in this work. Both approaches lead to the same wind-speed-free dependence (3.7), (3.8). Independent estimates of the physical invariants also give remarkably close values of $\alpha_{0(d)}$ and $\alpha_{0(f)}$. This can be considered as a positive validation of our approach.

4. Simulations of wind-wave growth

In this section we make use of numerical simulation results by Badulin *et al.* (2002, 2005, 2007*a*, 2008) and Zakharov *et al.* (2012) for verifying the above theoretical

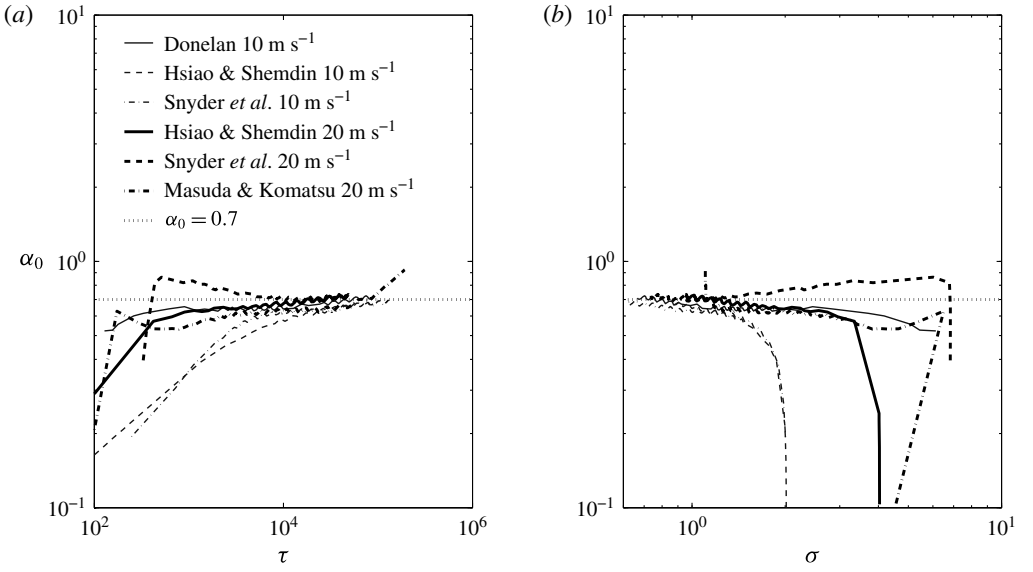

FIGURE 2. Dependence of parameter $\alpha_0 = (\mu^4\nu)^{1/3}$ (1.4) on: (*a*) non-dimensional duration $\tau = tg/U_{10}$ and (*b*) inverse wave age $\sigma = \omega_p U_{10}/g$ in simulations of duration-limited wind wave growth by Badulin *et al.* (2002, 2005, 2007*b*, 2008). Simulation setups (wind input parameterization and wind speed, e.g. table 6 of Badulin *et al.* 2005 for details) are given in the legend. The horizontal dotted line shows theoretical value $\alpha_{0(d)} = 0.7$.

results both in terms of the invariant (1.4) and the single-parametric dependencies of wave height on period (3.7), (3.8). The details of the corresponding numerical approaches can be found in the cited papers.

4.1. *Duration-limited growth*

The results of simulations (e.g. Badulin *et al.* 2005) are used here for verification of the law (1.4) for duration-limited wave growth. Figure 2 presents somewhat eclectic dependence of the wind-free invariant $\alpha_0 = (\mu^4\nu)^{1/3}$ on non-dimensional duration $\tau = tg/U_{10}$ (figure 2*a*) and inverse wave age $\sigma = \omega_p U_{10}/g$ (figure 2*b*). Wave input functions and wind speed values are shown in the legends. The straight line $\alpha_{0(d)} = 0.7$ is shown as a reference. All the simulations except the last one (our reproduction of the case by Komatsu & Masuda 1996) have been carried out with a primitive dissipation function associated with a hyper-dissipation at high frequencies (see Badulin *et al.* 2005). In these cases there is no saturated (fully developed or mature) wind-sea state and all the dependences are tending to $\alpha_{0(d)} \approx 0.7$ in full agreement with the results of § 2. The inverse wave age $\omega_p U_{10}/g$ can be considerably less than unity, i.e. nonlinear interactions support the growth of waves that can propagate significantly faster than wind (Glazman 1994).

To describe wave dissipation Komatsu & Masuda (1996) used the more sophisticated 'white-capping' function by Hasselmann (1974) (see also Komen, Hasselmann & Hasselmann 1984). In this case, wave height and period tend to their limits at large time. This feature is evidenced by a break of the dependence from the general tendency at inverse wave age $\omega_p U_{10}/g \lesssim 1$ in figure 2. Wave steepness μ and frequency ω_p are then approaching the limiting values while time t and, evidently, number of waves ν continue to grow.

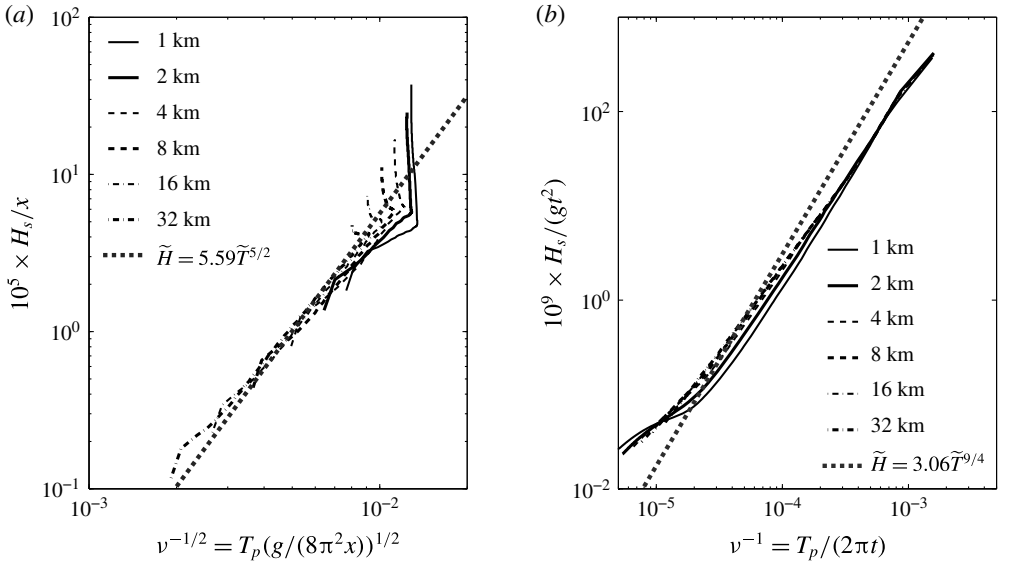

FIGURE 3. Wave growth curves in simulations of the fetch-limited setup (Zakharov *et al.* 2012) with: (*a*) fetch scaling (3.1) and (*b*) duration scaling (3.2). Curves are given for fixed fetches 1, 2, 4, 8, 16, 32 km (see legends). Theoretical dependences (3.7) and (3.8) are shown by dotted lines.

4.2. *Simulations of fetch-limited growth*

The fetch-limited growth has been simulated by Zakharov *et al.* (2012) starting from an initial white-noise spatially homogeneous wave field in a fetch interval 0–41 km and for times up to 385 000 s (approximately 107 h). Strictly speaking, there is no classic fetch-limited regime as a stationary state in these simulations. The evolution looks like a sequence of stages where reference dependences (3.7), (3.8) describe intermediate asymptotics. Figure 3 presents these results in terms of dependence on time at fixed fetches. Curves for log-spaced fetches 1, 2, 4, 8, 16 and 32 km are shown.

Figure 3(*a*) shows the evolution of wave parameters for wind-free scaling from the lower left to upper right corner and demonstrates an impressive coincidence with the 5/2 power law (3.8) over a wide range. Deviations from this dependence are seen at small dimensionless periods $\tilde{T}$ (short times, lower left in figure 3*a*) when wave spectra are far from self-similarity. For longer periods $\tilde{T}$ (longer times, upper right in figure 3*a*) a saturation of the wave field is reflected in the vertical asymptotes of the curves: wave periods (both dimensional and dimensionless) tend to their finite limits while wave heights continue to grow. This effect is probably associated with a simulation setup where the waves are modelled in a finite spatial box. At long times when the quasi-stationary state is reaching the upper bound of the box, the quasi-stationary fetch-limited growth then gives way to a duration-limited scenario.

The time-scaled representation (3.2) in figure 3(*b*) traces the wave evolution in an opposite sense when compared with figure 3(*a*): both $\tilde{H}$ and $\tilde{T}$ are decreasing with time. Curves plotted for different fetches appear to be remarkably close to each other and fit the theoretical tangent 9/4 in a range of more than one decade of $\tilde{T}$. For small dimensionless periods $\tilde{T} < 2 \times 10^{-5}$ and, correspondingly, long times and a large number of waves ($\tilde{T} \sim \nu^{-1}$), the saturation of wave field growth is evident as curves

deviating well above the reference dependence (3.7), counterparts of the saturation stage in figure 3(*a*). Thus, the wind-free relationships $\tilde{H}(\tilde{T})$ (3.7), (3.8) provide a good reference for the physical analysis of wave evolution.

5. Wind-wave growth in field experiments

In this section we investigate the invariance of wind-wave growth expressed by (1.4) for a collection of field experiments on wind-wave growth. First, we consider a number of experimental works since the milestone work by Sverdrup & Munk (1947) and then proceed with *in situ* data of wave riders of the Field Research Facility available from 1997 to the present (http://www.frf.usace.army.mil/frf_data.shtml).

5.1. *Classic experiments on duration- and fetch-limited growth*

As discussed in Hwang & Wang (2004), two classes of ocean wave measurements are of great importance for the study of the generation of ocean waves by wind. The first class is the fetch-limited growth condition, under which the wave development is limited by the available spatial coverage upwind of the measurement location. Over the years, there have been several successful field experiments reported. Extensive reviews and analyses of these datasets have been reported previously (e.g. Kahma & Calkoen 1992, 1994; Young 1999; Hwang & Wang 2004; Hwang 2006; Badulin *et al.* 2007*a*; Hwang *et al.* 2011).

The second class is the duration-limited growth condition, under which the wave development is limited by the temporal duration of the steady wind event acting on the water surface. The ideal initial and boundary conditions satisfying the duration-limited wave growth rarely occur in nature and it is no wonder that reports of such data are very scarce. Young (1999) presents an extensive review of fetch- and duration-limited wave growth studies. The only duration-limited datasets cited are Sverdrup & Munk (1947), Bretschneider (1952*a*,*b*) and Darbyshire (1959), as compiled by Wiegel (1961). DeLeonibus & Simpson (1972) report field data that contain duration growth information. Liu (1985) describes an interesting episode of almost 60 hours of quasi-steady wind forcing of wave growth measured by an NDBC wave buoy in Lake Superior. All these data are obtained at later stages of wave development with dimensionless time, $\tau = gt/U_{10}$, greater than about 7000. By chance, Hwang & Wang (2004) obtained one data set describing the duration growth in the first two hours of wind-wave generation and extended the data coverage by more than one order of magnitude (τ between 498 and 8801).

For our quantitative analysis, the fetch or duration data sets require information on the complete triplets of (ε, σ and τ) or (ε, σ and χ). We have been able to assemble in figure 4 nine fetch-limited data sets (Burling 1959; Hasselmann *et al.* 1973; Dobson, Perrie & Toulany 1989; Babanin & Soloviev 1998; Donelan 1979; Merzi & Graf 1985; Garciá-Nava *et al.* 2009; Romero & Melville 2010, the first five data sets are called collectively BHDDB, and the others D79, M85, G09 and R10 respectively), and three duration-limited data sets (DeLeonibus & Simpson 1972; Liu 1985; Hwang & Wang 2004, referred to as D72, L85 and H04).

In keeping with the conventional observation that the wave growth can be fitted by power-law functions (1.3) but allowing the exponents to vary with the range of dimensionless fetch or duration in different experiments, Hwang & Wang (2004) developed a second-order fitting of the power-law functions to the BHDDB

fetch-limited data and obtained (cf. (1.3), notation is slightly modified compared with Hwang & Wang 2004)

$$\varepsilon = \varepsilon_{0\chi}\chi^{p_\chi(\chi)}, \tag{5.1a}$$

$$\sigma = \sigma_{0\chi}\chi^{-q_\chi(\chi)}, \tag{5.1b}$$

where the exponents are slowly varying functions of dimensionless fetch χ given by

$$p_\chi(\chi) = \alpha_1 + 2\alpha_2 \ln\chi, \tag{5.2a}$$

$$q_\chi(\chi) = \beta_1 + 2\beta_2 \ln\chi, \tag{5.2b}$$

with $\varepsilon_{0\chi} = \exp(-17.6158)$, $\alpha_1 = 1.7645$, $\alpha_2 = -0.0647$, $\sigma_{0\chi} = \exp(3.0377)$, $\beta_1 = 0.3990$, and $\beta_2 = -0.0110$. A sufficient range of the dimensionless fetch χ for computation is 10^0–10^6.

Excluding fetch χ in (5.2*a*,*b*) one has a counterpart of the linear link (2.12) for self-similar solutions of the model (2.2)

$$q_\chi = \frac{2P_\chi p_\chi + S_\chi}{10}, \tag{5.3}$$

where

$$P_\chi = 0.8501, \quad S_\chi = 0.9900 \tag{5.4a,b}$$

are remarkably close to the theoretical value of unity. The duration-limited growth functions can be derived from a similar approach using a formal conversion of fetch x to time t (see Hwang & Wang 2004, for details). Trivial algebra leads to a similar relationship between p_τ and q_τ (cf. (2.7) and (5.3)), i.e.

$$q_\tau = \frac{2P_\tau p_\tau + S_\tau}{9}, \tag{5.5}$$

where the values of coefficients P_τ, S_τ

$$P_\tau = 0.8492, \quad S_\tau = 0.9889, \tag{5.6a,b}$$

again, appear to be quite close to the theoretical value of unity. The empirical fits (5.3), (5.5) and their theoretical counterparts (2.7), (2.12) are shown in figure 1.

One can examine the correspondence between the theory and the empirical knowledge by following the notes in the Introduction. After excluding wind speed from (1.3) one can easily obtain 'empirical' invariants (1.7):

$$\mu^4\nu^{r_\tau} = \text{const}_\tau, \quad \mu^4\nu^{r_\chi} = \text{const}_\chi \tag{5.7a,b}$$

in which exponents r_τ, r_χ depend on growth rates p_τ (p_χ). Generally, these exponents are close to unity as predicted by our theory (see (1.4)) but can vary in a wide range, even being negative for high exponents p_τ, p_χ.

An alternative formulation of the results allows tracing of the effect of fetch as follows:

$$(\mu^4\nu) = \varepsilon_{0\chi}^2\sigma_{0\chi}^{10}\chi^{-0.5391+0.0194\ln\chi} = \alpha_0(\chi)^3. \tag{5.8}$$

The additional dependence on dimensionless fetch χ yields a variation of α_0 in (5.8) by a factor 2.3833 when dimensionless fetch varies over a range of five orders of magnitude, $\chi = 10$–10^6. Figure 4 show the results of these field measurements similarly to figure 2 for simulations. The theoretical reference value of α_0 is reasonably consistent with experimental data and with the empirical fitting (5.8) by Hwang & Wang (2004). Typically, the duration-limited data show larger scatter, reflecting the departure from ideal duration-limited wave generation conditions as discussed at the beginning of this section.

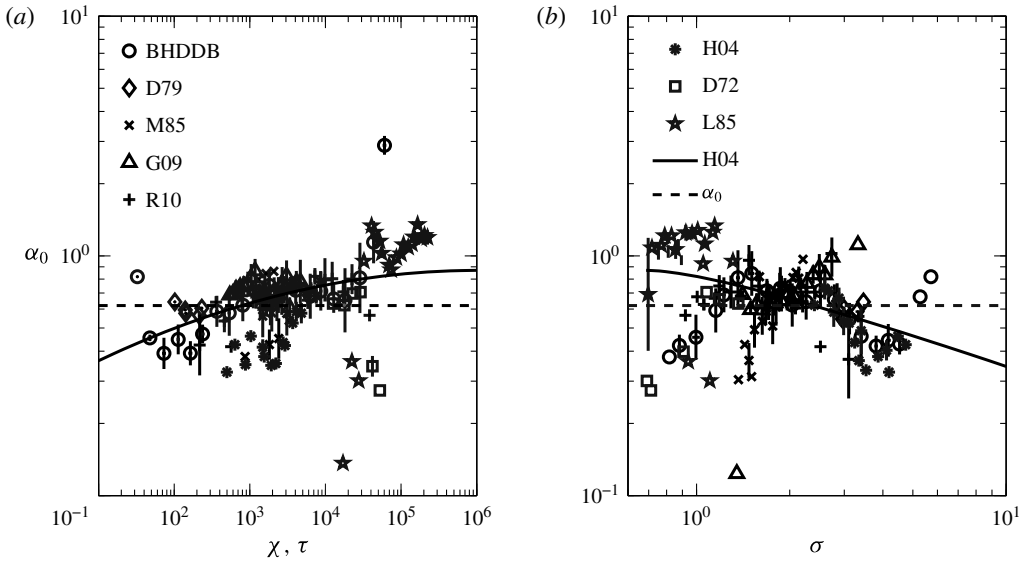

FIGURE 4. Dependence of experimental estimate of self-similarity parameter α_0: (*a*) on non-dimensional fetch $\chi = xg/U_{10}^2$ and duration $\tau = tg/U_{10}$; (*b*) on non-dimensional frequency of spectral peak $\sigma = \omega_p U_{10}/g$, for a combined collection of duration- and fetch-limited datasets. The dashed line shows the theoretical value $\alpha_{0(f)} = 0.62$, the solid line is the empirical power-law fit (5.8) by Hwang & Wang (2004) for the collection.

5.2. *Data by Sverdrup & Munk (1947)*

The special attention we pay to the work by Sverdrup & Munk (1947) is not limited to the historical aspects of wind-wave studies. The theoretical construction of their paper is quite close to our physical approach. Ten years before the formulation of the spectral approach for wind waves Sverdrup & Munk (1947) showed that 'the concept of 'significant waves' is essential for purpose of forecasting'. They started their theory from the equation for the integral balance of energy (see (47) in Sverdrup & Munk 1947), i.e. the counterpart of the second equation of our model (2.2). The effect of nonlinear interactions has been described by a semi-empirical relationship between two dimensionless parameters: wave steepness and wave age. The experimental data available at that time have been used to specify parameters of their model.

Figure 5 presents the data of tables II and III of appendix II by Sverdrup & Munk (1947). Only measurements containing full triads of wave height, period and fetch (duration) were taken into account. The upper row shows fetch- (figure 5*a*) and duration-limited (figure 5*b*) data with the conventional wind speed scaling. There is a rather large scatter of data around Toba's 3/2 law (dotted line). Strong deviations from Toba's law are associated with four particular data groups: US Eng. and Cornish for fetch- and Krümmel, Dover for duration-limited observations.

The alternative wind-free scaling plots in figure 5(*c*,*d*) also show large deviations from the reference dependences (3.7), (3.8) but the ranges of the corresponding dimensionless values are wider, especially, for the duration-limited case (figure 5*d*). Again, we can notice a clear disparity of points associated with the source of data and the method of estimating wave parameters. The data of USS Augusta and Gibson (fetch-limited) and of USS Augusta and Berkeley (duration-limited) show better agreement with theoretical dependence (dotted lines). The wave period in these

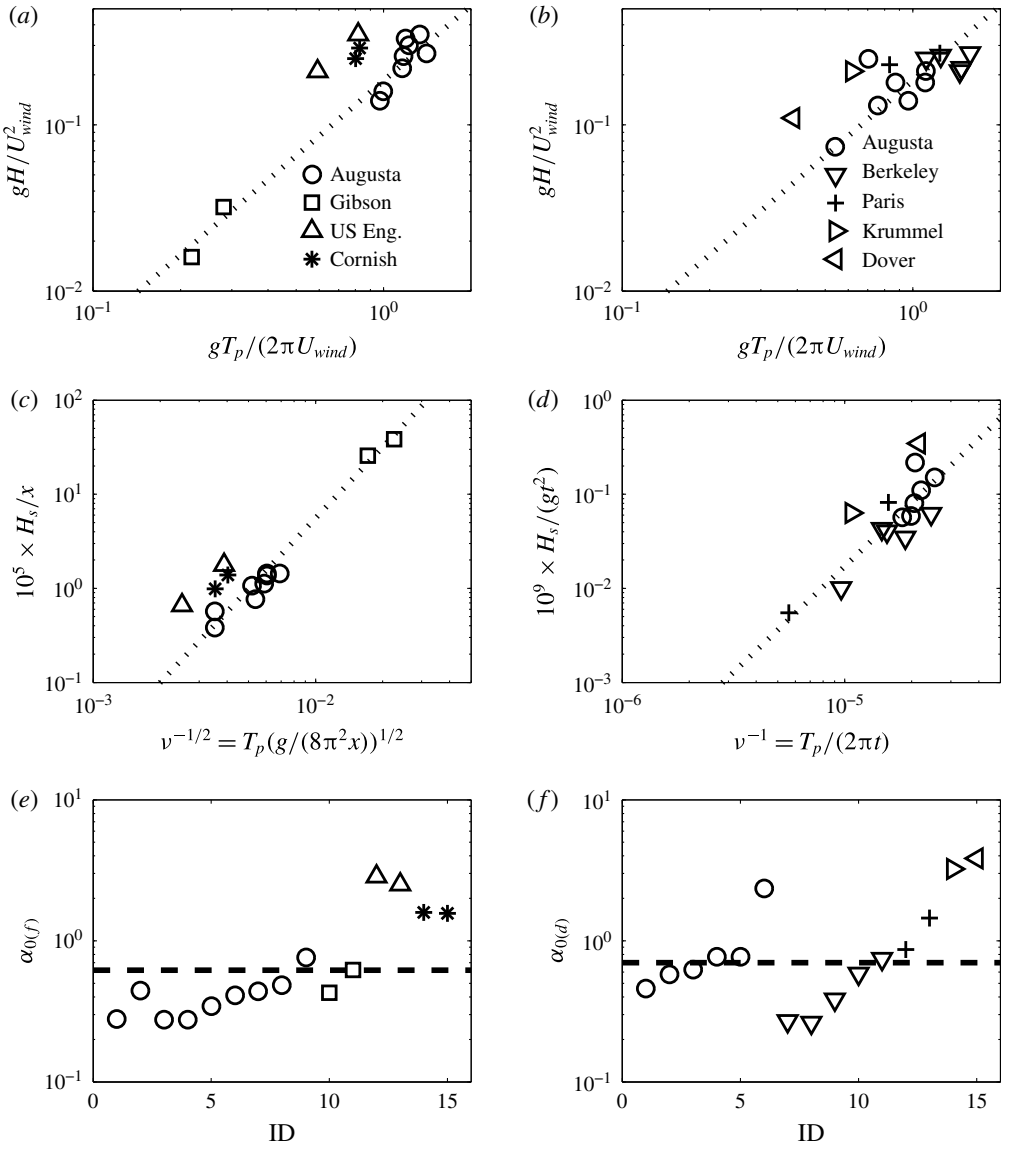

FIGURE 5. Data by Sverdrup & Munk (1947): (*a*,*b*) wave height–period dependence with the conventional wind speed scaling; (*c*,*d*) $\tilde{H}(\tilde{T})$ scaled by fetch (*c*) or time (*d*); (*e*,*f*) estimates of invariants $\alpha_{0(f)}$ and $\alpha_{0(d)}$. The dotted lines in (*a*–*d*) show the Toba (1972) law, and the dashed lines in (*e*,*f*) our theoretical values of $\alpha_{0(f)}$ and $\alpha_{0(d)}$. ID in (*e*,*f*) corresponds to records' ID in tables of Sverdrup & Munk (1947). (*a*,*c*,*e*) Data of table II for fetch-limited cases; (*b*,*d*,*f*) data of table III for duration-limited cases. Names of observation ship and authors are given in the legends of (*a*,*b*).

observations was estimated directly whereas those of Krümmel and Paris have been computed from measurements of wavelength.

The data in figure 5(*c*,*d*) cover the same range of dimensionless $\tilde{T}$ and $\tilde{H}$ as the simulations by Zakharov *et al.* (2012) in figure 3. One point of duration-limited data

Buoy ID	Fetch (m)	Wave direction (deg.)	Total number of data points	Number of points of off-shore waves
190	6112	320	23 772	102
192	18 500	260	20 526	35
200	18 500 × 3	280	5 773	24
430	18 500	250	70 995	606
630	3000	250	184 195	171

TABLE 1. Summary of wave rider data of the Field Research Facility of the US Army Corps of Engineers. Wave direction is reported as the direction from which the waves originate, e.g. waves coming from the west have direction 270°.

(figure 5*d*, Paris) appears below the lower limit of $\tilde{T}$ in figure 3(*b*), i.e. in the range we treated as a saturated wave field (see comments in § 4.2). As the opposite extreme, note the data of Gibson that fit both approaches (Toba's and the new one) fairly well (cf. figure 5*a*,*c*). Two points of Gibson correspond to very young waves in terms of wind speed scaling (wave age $C/U_{10} = 0.22$ and $C/U_{10} = 0.28$, see figure 5*a*). Short fetches (1.3 and 3.5 km) put these points into the upper right corner of figure 5(*c*). In terms of the 'life distance' x/λ, these points correspond to approximately 152 and 267 wave periods.

The bottom row, figure 5(*e*,*f*) demonstrates a surprising correspondence of the experimental estimates of the invariant α_0 to our theoretical values. Again, data of USS Augusta, Gibson and Berkeley give the best fit to $\alpha_{0(d)} = 0.7$ and $\alpha_{0(f)} = 0.62$. The agreement is considered quite good given the relatively poor quality of these early data sets.

5.3. *Data of the field research facility wave riders*

The data of wave riders in a near-shore area look very attractive for illustrating the law (1.4) in terms of the dependence of wave height on wave period (3.8). This simple 5/2 power-law dependence is verified with data available at the website of the Field Research Facility of the US Army Corps of Engineers http://www.frf.usace.army.mil/. A summary of the data is given in table 1. The wave riders collected data for many years; for example, Buoy 630 has been operational since 1997 and Buoy 430 since 2008. The most recent data downloaded for this analysis are dated September 2013. The total number of measurements and the number of data points relevant to the fetch-limited setup are listed in table 1. We have selected records when offshore wind direction was ±30° from the coast normal. Buoy 200 is sheltered by a cape from the north; this is the closest coastline but there is almost no wind from that direction. Direction 280° has been taken as an alternative reference and the corresponding fetch has been set as three times longer than the one from the closest shoreline.

Wind from the ocean is dominating in this area and only 0.31 % of total number of data points (938 of 305 261) qualifies as consistent with a fetch-limited setup of wave growth. When presented in dimensionless variables (3.1) these data match the theoretical dependence $\tilde{H}(\tilde{T})$ (3.8) fairly well as seen in figure 6. The data of the buoys cover a wide range of dimensionless periods ('life distances'), similar to figures 2–5 for simulations of wave growth, more recent wave growth data reported in Hwang & Wang (2004) and the historical data by Sverdrup & Munk (1947). A slight overshoot relative to the theoretical dependence can be explained by a systematic

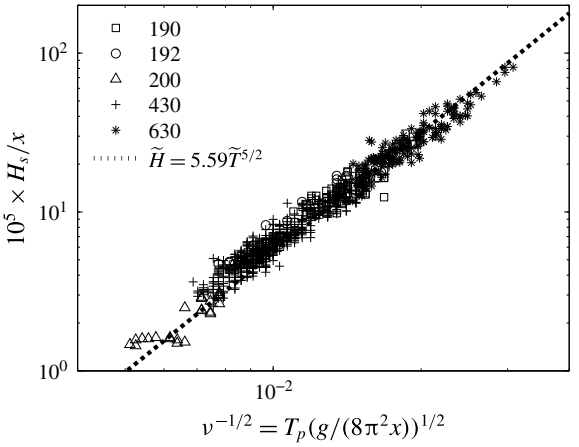

FIGURE 6. Data of Field Research Facility wave riders versus theoretical dependence (3.8) shown as dotted line. Different buoy data are shown by different symbols (see legend and table 1).

underestimating of wave periods. Underestimating of fetch can also contribute to this overshoot when the wave development is slowed down by the coast sheltering effect. The scaling gives a good approximation for the problem of wave growth at relatively small slanting fetches, for our present knowledge up to 40° from the coastline normal. At larger angles the wave growth off-shore is accompanied by a complex system of along-shore modes as shown in recent simulations of fetch-limited growth in which the effect of nonlinear wave–wave interactions has been accounted for in full (e.g. Gagnaire-Renou 2009; Zakharov *et al.* 2012).

6. Wind-wave growth observed in laboratory experiments

It is commonly admitted that the dynamics of water waves observed in wind-wave tanks differ dramatically from those of wind waves observed in open seas. Most of the experimental facilities are considered as too short for reaching the full development of wave–wave interactions and for observing the related statistical properties of wind-wave fields. At the same time, a number of laboratory results have been generalized successfully for *in situ* wave field conditions. Examining a set of wind-wave field data obtained in the laboratory in a wide range of fetch and wind conditions according to the approach developed in this paper may help to clarify, at least partly, the soundness of this viewpoint.

In this section, we consider the results of two experiments made in two different wind-wave tanks. Experiments in the early 1960s by Toba (1961) served as a basis for later works on the famous 3/2 power law by Toba (1972, 1973*a*,*b*) that links dimensionless wave height and wave period.

The observations reported by Caulliez, Makin & Kudryavtsev (2008), Badulin & Caulliez (2009) and Caulliez (2013) were made in the large wind-wave tank in Marseille for various fetches between 2 and 26 m (i.e. 2, 4, 6, 9, 13, 18 and 26 m) and 10 wind speeds (values given in the legends of figure 7). Measurements of wind and wave parameters are based on much more advanced technology and methodology, allowing a proper examination of wind-wave development both within the conventional wind scale approach and the above-presented theory.

6.1. *Wind speed scaling in experiments by Toba (1961, 1972) and Caulliez et al. (2008) and Caulliez (2013)*

Figure 7(*a*) shows the classical representation of wind-wave growth in terms of the dimensionless wind-dependent wave parameters H^* and T^*, using the definitions based on wind friction velocity as given by Toba (1972). The whole sets of data obtained respectively by Toba (1972, table 1 therein, filled symbols) and by Caulliez (2013, partially given in table 1, open symbols) are displayed. In particular, the Toba and Caulliez data were collected for a number of similar conditions, namely for reference wind speeds between 5 and 12 m s^{-1} and fetches between 6 and 14 m but in facilities of quite different sizes, the water tanks being respectively 21 and 40 m long.

In addition, the air layer above Toba's water tank was just 50 cm in height $\times$ 75 cm in width and, clearly, the air flow above waves might be affected by the walls. The wind friction velocity was determined from the mean velocity profiles measured at three fetches by means of small cup anemometers while the significant wave height was derived from the mean wave height estimates. When compared to the Marseille data as given in Caulliez *et al.* (2008) and Caulliez (2013), the original data reported by Toba (1972) in figure 7(*a*) show laboratory waves 'unrealistically young' exhibiting abnormally small T^* associated with inverse wave age in the range 20–45, i.e. propagating 20–45 times slower than the wind speed estimated at the standard 10 m level (note that for short gravity waves, when neglecting drift current effects on wave propagation, T^* corresponds approximately to 2π times the wave age C/u_*). A thorough examination of the data set has shown such very small values of wave age are related to abnormally high values of friction velocity.

The observations reported by Caulliez (2013) in the large wind-wave tank in Marseille were made for a wider range of wind speeds and fetches, from 2 m up to 26 m, with an air layer above the water surface of 1.5 m in height and 3.2 m in width. The friction velocity was determined from careful hot-X-wire measurements of the vertical profiles of the turbulent momentum flux in air, a quantity found constant within the whole water surface boundary layer (Caulliez *et al.* 2008). The significant wave height was estimated as four times the root-mean-square value of the water surface displacements. In this experiment, the inverse wave age varied between 4 and 18.

In figure 7(*a*), data sets by both Toba and Caulliez follow quite well the Toba 3/2 power law. However, the Toba data are strictly separated from the Caulliez ones in the range of wave age T^* observed. Additionally, all the Toba data are quite close to the 3/2 power law while the Caulliez data observed at the shortest fetches, in a range depending on wind speed (up to 26 m at 2.5 m s^{-1} to less than 6 m at 10 m s^{-1}) show a transition to a 'saturated wave field state', in the words of Toba (1972). These transitional points of the Caulliez data appear as outliers from the ones of Toba collected in the same range of wave age and fetches (e.g. between 6 and 14 m).

Therefore, Toba's data have been re-analyzed by using more realistic values of wind and wave parameters based on the detailed measurements made in the large Marseille wind-wave tank. In brief, new friction velocity values have been derived from drag coefficient estimates obtained in Marseille at the same fetches and reference wind speeds as Toba's data. Note that these new values are in very good agreement with the u_* values measured by Kawai (1979) in a wind-wave tank of size comparable to the tank used by Toba (1961) in the experiments analyzed here. In addition, significant wave height has been evaluated from the mean wave height given by Toba (1972) on the basis of the wave height probability distribution observed in Marseille and

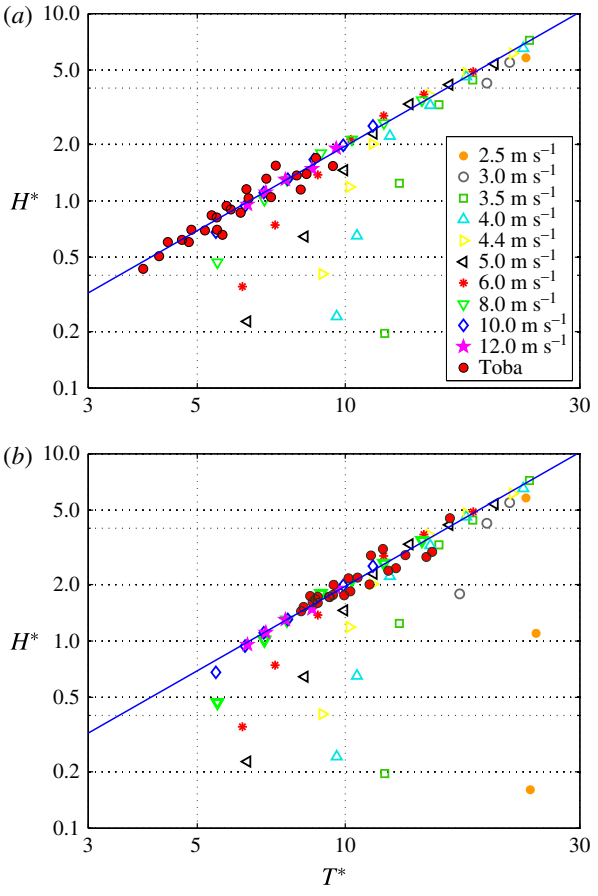

FIGURE 7. Data of wind-wave tank studies of wave growth by Toba (1972) (filled symbols) and by Caulliez (2013) (open symbols) made dimensionless by using the gravity parameter g and the conventional friction velocity $u^* = \langle U'W' \rangle^{1/2}$ ($T^* = gT/u^*$ and $H^* = gH_s/u^{*2}$). (*a*) Toba's data derived from table 1 in Toba (1972); (*b*) friction velocity values u^* given in Toba (1972) are replaced by estimates at the same reference wind speed and fetch made on the basis of the Caulliez measurements in the large Marseille wind wave tank. Solid line is the Toba (1972) 3/2 law.

not from the Rayleigh distribution generally assumed for *in situ* conditions (see for instance figure 9 in Caulliez *et al.* 2008). When these new parameters are used for estimating T^* and H^*, it is striking to see in figure 7(*b*) that both data sets again agree very well but now, in a more realistic way, fall into the same range of wave age T^*. As previously mentioned, they also follow remarkably well the 3/2 power law except for the non-saturated wave fields observed at the shortest fetches.

6.2. *Wind-free scaling in experiments by Toba (1961, 1972) and Caulliez (2013)*

Figure 8 shows the same data sets obtained by Caulliez and Toba but plotted with the new scaling representation (3.1) based on the law of universality (1.4). For Toba's data in figure 8, the significant wave height has been estimated in the same way as in figure 7(*b*). The correspondence between the two experimental data sets and the

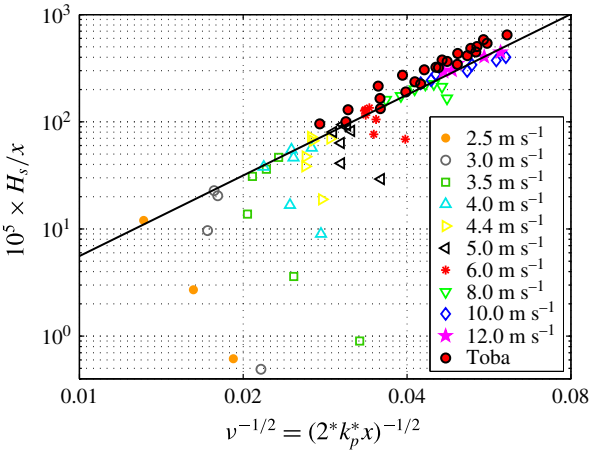

FIGURE 8. Data derived from wind-wave tank studies of wave growth by Toba (1972) (filled symbols) and by Caulliez (2013) (open symbols) plotted in terms of the new scaling (3.1). Solid line is the Toba (1972) 3/2 law.

theoretical 5/2 power-law dependence (3.8) looks very good for the well-developed wave fields observed at the largest fetches, but the experimental points of Toba (1972) are located about 1.5 times higher than the theoretical curve given by (3.8). This overshoot may be explained by the use of different methods for estimating the spatial wave period $\tilde{T}$ as given by (2.19) and (3.4).

For fetch-limited conditions, as seen from (2.19), the dimensionless spatial wave period is a measure of the number of waves propagating over the fetch distance x, i.e. $\tilde{T} = (2|\boldsymbol{k}_p|x)^{-1/2}$. In the Toba (1972) experiments based on one-point wave gauge measurements, wave period was first derived from the mean-over-spectrum or dominant peak time scale and the related spatial quantity $\tilde{T}$ was estimated by using the linear dispersion relation for gravity waves. Caulliez (2013) however measured directly the phase speed C_p of dominant waves by means of a cross-correlation method between two wave signals recorded by a pair of wave gauges (Dudis 1981). This method enables direct measurement of the velocity of wave propagation accounting for the effect of surface drift current and, for the shortest waves, the effect of surface tension. In the observations reported here, the magnitude of these combined effects varies between 70 % of the linear phase velocity value for small fetches and wind speeds, to 10 % for large fetches and winds. This clearly indicates that the dynamics of wind-wave fields observed in the laboratory are governed not only by the gravity force but also by surface drift and, at the shortest scales, by capillary forces.

The good agreement observed in figure 8 between the Caulliez (2013) data at large fetches and the theoretical curve given by (3.8), in contrast to the Toba (1972) data, validates the use of this experimental method for estimating $\tilde{T}$ for wind-wave tank observations. This noticeable fit also supports the appropriateness of the new scaling approach for describing well-developed wind-wave fields observed in laboratory at large fetches.

Finally, figures 7 and 8 enable us to consider two issues thoroughly: the success of the new approach for wind-wave tank observations and the related relevance of the conventional wind speed scaling under Toba's law. To support this viewpoint, one can also notice that, in figure 8, the range of dimensionless periods $\tilde{T}$ observed at

the smallest wind speeds overlaps the data of the Field Research Facility for buoys 190 and 630 located at the minimal distances from the coast, i.e. at 3 and 6 km respectively (see figure 6). The equivalent dimensionless fetch in terms of wavelength – the number of waves ν – for the wind-wave tank data can be estimated as 50 to 300, i.e. values quite close to those obtained by Gibson ($\tilde{T}$ is 152 and 266 at fetches 1.3 and 3.5 km and wind speeds 16.5 and 16 m s^{-1} respectively) described in our analysis of the Sverdrup & Munk (1947) results. Thus, with the new approach one can see that wind waves of lengths higher than roughly 15 cm observed in large water tanks are developed enough to be considered for modelling the nonlinear interactions and statistical properties of the resulting wave field.

6.3. *Toba's law and the wind-free approach: similarities and dissimilarities*

The data presented here and in the previous sections (see figure 5 for data by Sverdrup & Munk 1947) show quite good correspondence of the observations both with our theoretical dependences and with Toba's power law, especially for wind-wave tank experiments. It reflects, in a sense, the similarities between the basic physical assumptions of both the purely theoretical model described here and the theoretical–empirical model by Toba (1972). Both models consider physical mechanisms providing a local balance (as emphasized in the title of the paper by Toba 1972).

Toba (1972) develops his model using a dimensional analysis, associating the wave energy growth rate with the work of the wave-induced wind stress in the field of wave orbital motions. Assuming that this work is directly controlled by the local air flow (and not by wave parameters), and then is proportional to u^{*3}, he derived the so-called 3/2 Toba relationship between the dimensionless wave height and wave period. Note that this law is equivalent to proportionality of the total drift current including the Stokes one (i.e. the averaged value of the orbital velocity) and the friction velocity u^*. This relation that links the wave steepness to the root-mean-square of the inverse wave age expresses the local equilibrium of the dominant wind-wave field but here the treatment is heuristical rather than theoretically well-grounded.

One of the reviewers pointed out that the Stokes drift current is an essentially nonlinear effect of second order in the wave steepness and, thus, unrelated to viscosity and to friction velocity: it is present in a nonlinear wave field in the absence of wind as well. The Stokes drift current therefore can be easily observed in laboratory flumes where waves are generated mechanically by a wavemaker. In the present use of the terminology (of Stokes drift), we mean a somewhat different contribution to the total drift current that results from the shear stress on the air–water interface due to the presence of wind. Interestingly, in laboratory wind-wave facilities these two different contributions to the drift current at the water surface are often of comparable magnitude.

On the contrary, in the present theoretical model we assume the nonlinear interactions to be dominant compared to the external forcing terms S_{in} and S_{diss} and exploit the key features of nonlinear transfer among the random water wave field components explicitly. The remarkable fact is that one can express the corresponding balance of the wave field energy (or momentum, or action) in terms of wave parameters only, without any reference to wind forcing and/or dissipation. However, when examining this model in terms of the dependence of wave height on wave period, this balance gives the Toba 3/2 law but as an important special case of local wave field equilibrium for which the flux of energy to waves (or the 'rate of work

done by the wind stress to wind waves' in the words of Toba 1972) remains constant. Furthermore, as shown in Gagnaire-Renou *et al.* (2011), the wave energy growth rate can be expressed as a function of u^{*3}. The present model thus leads to expressing the strong assumption made by Toba (1972) as the result of the predominance of nonlinear interactions among the other processes governing the wind-wave field evolution. It also means that, in this case, both models represent very similar physics, but here our model reveals more precisely the governing physical mechanisms.

The mathematically consistent analysis of the model (2.2) allows the effect of dominating nonlinearity to be accounted for in a quite 'flexible' way as two-parametric families of self-similar solutions (2.6), (2.11) and, thus, a description of energy flux that depends on time or fetch. The 'freedom' of these solutions comes from homogeneity properties (2.3), i.e. from arbitrariness of physical scaling of deep-water wave lengths and heights (coefficients υ and ϱ in (2.3)). It allows the balancing of the dominating nonlinear wave transfer and the total net input (see (2.2*b*)) in a wide range of physically relevant wind-wave growth scenarios when energy income depends on time or fetch. On the contrary, the restrictiveness of Toba's model is inherently associated with the definite physical scale of wind speed. Toba fixes this scale by postulating that 'the growth of wind waves is predicted by an integration with respect to the fetch and duration' (Toba 1972, p. 18) and, hence, in fact, by freezing a particular scenario of wave development at constant energy growth rate.

A divergence of the two approaches is then observed beyond the quite restrictive Toba's wave growth scenario, i.e. when the energy flux to waves varies with time or fetch. The cases by Hasselmann *et al.* (1976) and Zakharov & Zaslavsky (1983) considered above (see also Gagnaire-Renou *et al.* 2011) provide other exponents in the dependence of wave height on frequency. In the context of this problem, the consistency between the 'wind-based' model by Toba and our 'wind-free' model, especially for wind-wave tank observations (cf. figures 7 and 8) might be the most striking manifestation of the 'universal' behaviour of wind–wave coupling occurring in the laboratory when external air and water flow disturbances are minimized. These conditions make the friction velocity u^* a fully representative physical parameter.

7. Discussion and conclusions

In this paper we revisit a variety of theoretical, numerical and experimental results obtained previously over several decades in order to examine in detail a new theoretical concept of wind-wave growth. This final section aims to show the inner consistency and logic of this reconsideration.

7.1. *Theory*

The key result of this paper is the invariant (1.4) of wind-wave field growth. The basic assumption of the dominating role of nonlinear wave transfer leads to the property of self-similarity of wind-wave spectra for the reference cases of duration- and fetch-limited wave growth and the power-law dependence of dimensionless wave parameters on fetch and time duration (1.3). In contrast to the traditional power-law fits with four free parameters, the theoretical analysis demonstrates the existence of rigid links between exponents and pre-exponents of (1.3). These universal links then give us the universal form of the invariant (1.4), (cf. (1.7)) with the right-hand-side α_0 being expressed by cumbersome integral dependences of spectral shape functions (e.g. Hasselmann *et al.* 1976). We assume α_0 to be constant based on previous experimental and numerical studies that showed spectral shape invariance of growing

wind seas. The ultimate result of these theoretical considerations implies a surprising conclusion that appears to contradict the present understanding of wind-wave growth: the invariant (1.4) does not contain wind parameters explicitly. In other words:

waves chronicle wind development.

This wind-free paradigm implies a new scaling of dimensionless wave height and period (3.7), (3.8): the simple time duration or fetch becomes a key physical scale irrespective of the conditions of wind forcing. We show that the new theoretical dependences agree fairly well with conventional theoretical–empirical ones (e.g. Hasselmann *et al.* 1976; Carter 1982). Exclusion of wind speed from these dependences gives exactly exponents 9/4, 5/2 and, what is more surprising, provides consistent estimates of basic constants $\alpha_{0(d)}$, $\alpha_{0(f)}$ (see (3.11)). In particular, the reference to the theoretical–empirical model by Hasselmann *et al.* (1976) is quite representative. The purely theoretical approach shows that the empirical estimations of the parameters in the JONSWAP spectrum and its specific spectral shape are, in a sense, exhaustive for the analysis: the results are substantiated by much more general physical principles.

7.2. *Simulations of wind-wave growth*

We stress that all the numerical experiments were accomplished almost ten years ago with no reference to our findings in this paper. A series of runs for a duration-limited setup from Badulin *et al.* (2005, 2007*a*, 2008) taken arbitrarily showed a very good agreement with the results of this new theory.

The recent numerical study of fetch-limited growth by Zakharov *et al.* (2012) gives us a broader view of the classic problem of wind-wave growth. We found that the fetch-limited regime is just an intermediate asymptotic stage when wave growth is limited in space. When waves from the coast arrive at the opposite side of the simulation domain the waves continue to grow but according to a duration-limited scenario.

7.3. *Field experiments on wind-wave growth*

Field studies of wave growth provide the dominant support for the new theory. First, we show that the parameters of the power-law experimental fitting (1.3*a*–*d*) are linked. The theoretical links (2.7), (2.12) reproduce the parameterizations by Hwang & Wang (2004) reasonably well: a minor quantitative difference makes the invariant (1.4) weakly dependent on dimensionless fetch (or wave age).

The outcome of our historical review of the brilliant paper by Sverdrup & Munk (1947) is two-fold. First, we show that the relatively coarse wave observations made during World War II are consistent with our theory. Secondly, we emphasize the parallel between our self-similarity approach and the concept of significant wave height. Both approaches describe the wave field with a minimal number of parameters: significant wave height and peak period, in contrast to the more detailed but much more expensive representation of wave field as an ensemble of a great number of spectral components.

Data from wave riders of the US East Coast were analyzed as an additional justification of these new theoretical outcomes. Wave heights and periods scaled by the new wind-speed-free parameterization show remarkable closeness to the 5/2 law for the fetch-limited case. We expect that more experimental proof of the validity of such an approach can be found in more wave data.

7.4. *Wind-wave tank experiments: beyond the formal validity of the statistical description?*

The results obtained from wind-wave tank experiments are found to be well representative. Even if the wind-wave tank experiments are generally considered as too far from wind-sea reality, careful data treatment enables one to show that it is probably not the case. In terms of the new wind-free scaling the results of experiments in the Large Air-Sea Interaction Facility (LASIF) in Marseille fit the theoretical dependences remarkably well. They correspond to high values of dimensionless $\tilde{H}, \tilde{T}$, i.e. those obtained at relatively short fetches. As expected, the statistical description used in this work may not apply in this case. At the same time, the range of wave age observed in the wind-wave tank experiments overlaps those observed by the wave riders. This finding affords promising perspectives for modelling sea waves in large wind-wave facilities (Zavadsky, Liberzon & Shemer 2013).

7.5. *A final remark*

Evidently, the invariant (1.4) does not provide a full description of wind-wave field evolution for the classic setups of duration- and fetch-limited growth. Essentially, it shows that the problem can be split into two steps and, in the first step, gives an essential physical constraint that does not contain any parameters of wind forcing. The effect of wind can be accounted for in the next step to get the full description of wave growth in terms of wave height and period as functions of time, fetch and parameters of wind–sea coupling.

Thus, the concise expression (1.4) shows the validity and prospects of an analytical theory of wind-driven seas. To a certain extent, this result breaks a long-lived belief that the description of wind-driven seas must be the subject of extensive experimental studies and costly simulations rather than the result of an elegant physical theory.

Acknowledgements

Sections 2–4 of the paper are supported by Russian Science Foundation N14-22-00174. Other parts of the work are sponsored by the Office of Naval Research (Naval Research Laboratory PE 61153N), ONR grant N000141010991, National Science Foundation N1130450 and the French Centre National d'Etudes Spatiales (TOSCA/SMOS-Ocean project). Authors are thankful for data provided by the Field Research Facility, Field Data Collections and Analysis Branch, US Army Corps of Engineers, Duck, North Carolina. The NRL publication number is NRL/JA/7260-14-0232. The authors are grateful to referees for their constructive and useful suggestions.

Appendix A. Self-similar solutions for growing wind seas

A.1. *Duration-limited case*

Let us consider the duration-limited case, i.e. a spatially homogeneous case where $\partial E/\partial x \equiv \partial E/\partial y \equiv 0$. Solutions for the conservative kinetic equation (2.2*a*) with homogeneity condition (2.3) can be found in the form of incomplete self-similarity (2.6).

After substituting (2.6) into (2.2*a*) one has

$$(p_\tau + 4q_\tau)\Phi_{p_\tau}(\boldsymbol{\xi}) + 2q_\tau \boldsymbol{\xi}\nabla_\xi \Phi_{p_\tau} = a_\tau^2 b_\tau^{-17/2}\tau^R S_{nl}[\Phi_{p_\tau}(\xi)], \tag{A 1}$$

where exponent $R = 2p_\tau - 9q_\tau + 1$ should be zero to cancel the explicit dependence on time τ and to leave a dependence on self-similar argument $\boldsymbol{\xi}$ only. It gives the linear link (2.7) between exponents p_τ and q_τ. An additional link between coefficients a_τ and b_τ (2.8) can be introduced by simple re-scaling of dimensionless variables. The total dimensionless energy for solutions (2.6) with (2.8) becomes

$$\tilde{E}_{tot} = \int\int_{-\infty}^{+\infty} a_\tau \tau^{p_\tau+4q_\tau} \Phi_{p_\tau}(\boldsymbol{\xi})\, \mathrm{d}\boldsymbol{k} = a_\tau^{9/17} \tau^{p_\tau} I_\tau \tag{A 2}$$

where

$$I_\tau = \int\int_{-\infty}^{+\infty} \Phi_{p_\tau}(\boldsymbol{\xi})\, \mathrm{d}\boldsymbol{\xi}. \tag{A 3}$$

Links (2.7), (2.8) are of key importance for further consideration. First, equation (A 1) for shape function $\Phi_{p_\tau}(\boldsymbol{\xi})$ with (2.8) depends on exponents p_τ, q_τ but appears to be independent of coefficients a_τ, b_τ. Secondly, the self-similar solutions (2.6) with the integral (A 2) depending on two parameters only (say, a_τ and p_τ) are consistent with a power-law dependence of net wave input on time in (2.2*b*).

A characteristic frequency ω_* can be introduced in different ways for a given spectral shape function $\Phi_{p_\tau}(\boldsymbol{\xi})$. The mean-over-spectrum frequency is written as follows:

$$\tilde{\omega}_m = \frac{\displaystyle\int\int_{-\infty}^{+\infty} \tilde{\omega} \Phi_{p_\tau}(\boldsymbol{\xi})\, \mathrm{d}\boldsymbol{\xi}}{\displaystyle\int\int_{-\infty}^{+\infty} \Phi_{p_\tau}(\boldsymbol{\xi})\, \mathrm{d}\boldsymbol{\xi}} = a_\tau^{-2/17} \tau^{-q_\tau} J_\tau I_\tau^{-1}, \tag{A 4}$$

where

$$J_\tau = \int\int_{-\infty}^{+\infty} |\boldsymbol{\xi}| \Phi_{p_\tau}(\boldsymbol{\xi})\, \mathrm{d}\boldsymbol{\xi}. \tag{A 5}$$

Peak frequency $\tilde{\omega}_p$ that corresponds to a maximum of the shape function $\Phi_{p_\tau}(\boldsymbol{\xi})$, evidently, has similar dependence on time and parameter a_τ

$$\tilde{\omega}_p = h_{p_\tau} \tilde{\omega}_m = h_{p_\tau} a_\tau^{-2/17} \tau^{-q_\tau} J_\tau I_\tau^{-1}, \tag{A 6}$$

where the coefficient $h_{p_\tau} < 1$ for wind-wave spectra: the mean frequency is generally higher than the peak one. Note that this coefficient depends on the exponent p_τ. Below we use the spectral peak frequency ω_p unless otherwise stated.

While total wave energy (A 2) and characteristic frequency (A 4), (A 6) are power-law functions, the exponents of which are linked by a linear relationship (2.7) one can construct easily a time-independent invariant in the form

$$\tilde{E}_{tot}^s \tilde{\omega}_p^y \tau = a_\tau^{9s/17-2y/17} \tau^{sp_\tau - yq_\tau + 1} I_\tau^{s-y} J_\tau^y h_\tau^y \tag{A 7}$$

by choosing appropriate exponents s and y. Exponents $s = 2$ and $y = 9$ cancel dependence on time τ in (A 7). One remarkable result is that this choice cancels dependence on parameter a_τ as well. Condition (2.7) on exponents p_τ and q_τ gives a time-independent invariant that depends on one parameter only of the family of self-similar solutions (2.6). The invariant (A 7) can be associated with the weakly turbulent law of wind-wave growth by Badulin *et al.* (2007*a*) in the form of the Kolmogorov relationship between energy and energy flux (total net input) (2.15). Finally, one has the invariant in a remarkably concise and physically transparent form in terms of wave steepness μ (1.5) and number of waves ν as defined by (1.6)

$$\mu^4 \nu = I_\tau^{-7} J_\tau^9 h_\tau^9 = \alpha_{ss(d)}^3 p_\tau = \alpha_{0(d)}. \tag{A 8}$$

Here we use subscript (d) for the duration-limited case.

A.2. *Fetch-limited case*

Self-similar solutions for a fetch-limited setup can be considered quite similarly to the duration-limited case. Assuming the wave field to be stationary ($\partial E/\partial t \equiv 0$) and growing in increasing x one has self-similar solutions in the form (2.11) and condition (2.13) is quite similar to the duration-limited case.

For dimensionless energy (cf. (A 2) with (2.13)) one has

$$\tilde{E}_{tot} = \int \int_{-\infty}^{+\infty} a_\chi \tau^{p_\chi + 4q_\chi} \Phi_{p_\chi}(\boldsymbol{\zeta})\, \mathrm{d}\boldsymbol{k} = a_\chi^{5/9} \chi^{p_\chi} I_\chi, \tag{A 9}$$

where

$$I_\chi = \int \int_{-\infty}^{+\infty} \Phi_{p_\chi}(\boldsymbol{\zeta})\, \mathrm{d}\boldsymbol{\zeta}. \tag{A 10}$$

The mean-over-spectrum frequency is written as follows:

$$\tilde{\omega}_m = \frac{\int \int_{-\infty}^{+\infty} \tilde{\omega} \Phi_{p_\chi}(\boldsymbol{\zeta})\, \mathrm{d}\boldsymbol{\zeta}}{\int \int_{-\infty}^{+\infty} \Phi_{p_\chi}(\boldsymbol{\zeta})\, \mathrm{d}\boldsymbol{\zeta}} = a_\chi^{-1/9} \chi^{-q_\chi} J_\chi I_\chi^{-1} \tag{A 11}$$

and the peak one as

$$\tilde{\omega}_p = h_{p_\chi} \tilde{\omega}_m = h_{p_\chi} a_\chi^{-1/9} \chi^{-q_\chi} J_\chi I_\chi^{-1}, \tag{A 12}$$

where

$$J_\chi = \int \int_{-\infty}^{+\infty} |\boldsymbol{\zeta}| \Phi_{p_\chi}(\boldsymbol{\zeta})\, \mathrm{d}\boldsymbol{\zeta}. \tag{A 13}$$

The fetch-independent invariant can be derived in the same way as the one for the duration-limited setup (A 7) and related with formulations by Badulin *et al.* (2007*a*), Gagnaire-Renou *et al.* (2011)

$$\tilde{E}_{tot} \tilde{\omega}_p^4 = \alpha_{ss(f)} \left(\frac{\tilde{\omega}_p^2}{2} \frac{\partial \tilde{E}_{tot}}{\partial \chi} \right)^{1/3}. \tag{A 14}$$

Finally, one has the invariant in terms of wave steepness μ (1.5) and number of waves in terms of wavelength

$$\nu = 2\boldsymbol{k}_p \boldsymbol{x}, \tag{A 15}$$

which is identical to the duration-limited case

$$\mu^4 \nu = I_\chi^{-8} J_\chi^{10} h_\chi^{10} = \alpha_{ss(f)}^3 p_\chi = \alpha_{0(f)}. \tag{A 16}$$

The right-hand sides of (A 8), (A 16) are formally different and are determined by self-similar functions $\Phi_\tau(\boldsymbol{\xi})$, $\Phi_\chi(\boldsymbol{\zeta})$.

REFERENCES

BABANIN, A. N. & SOLOVIEV, YU. P. 1998 Field investigation of transformation of the wind wave frequency spectrum with fetch and the stage of development. *J. Phys. Oceanogr.* **28**, 563–576.

BADULIN, S. I. 2010 ABC of wind wave growth. In *17th Conference Waves in Shallow Water Environment, Brest, France*, http://wave.ocean.ru/badulin/ABC_WISE2010.ppt.

BADULIN, S. I., BABANIN, A. V., RESIO, D. & ZAKHAROV, V. 2007*a* Weakly turbulent laws of wind–wave growth. *J. Fluid Mech.* **591**, 339–378.

BADULIN, S. I., BABANIN, A. V., RESIO, D. & ZAKHAROV, V. E. 2007*b* On experimental justification of weakly turbulent nature of growing wind seas. In *10th International Workshop on Wave Hindcasting and Forecasting and Coastal Hazard Symposium*, http://www.waveworkshop.org/10thWaves/ProgramFrameset.htm.

BADULIN, S. I., BABANIN, A. V., RESIO, D. & ZAKHAROV, V. 2008 Numerical verification of weakly turbulent law of wind wave growth. In *IUTAM Symposium on Hamiltonian Dynamics, Vortex Structures, Turbulence. Proceedings of the IUTAM Symposium held in Moscow, 25–30 August, 2006* (ed. A. V. Borisov, V. V. Kozlov, I. S. Mamaev & M. A. Sokolovskiy), IUTAM Bookseries, vol. 6, pp. 175–190. Springer.

BADULIN, S. I. & CAULLIEZ, G. 2009 Significance of laboratory observations for modeling wind-driven seas. *Geophys. Res. Abstracts* **11**, EGU2009–12694.

BADULIN, S. I. & GRIGORIEVA, V. G. 2012 On discriminating swell and wind-driven seas in voluntary observing ship data. *J. Geophys. Res.* **117**, C00J29; doi:10.1029/2012JC007937.

BADULIN, S. I., PUSHKAREV, A. N., RESIO, D. & ZAKHAROV, V. E. 2002 Direct and inverse cascade of energy, momentum and wave action in wind-driven sea. In *7th International Workshop on Wave Hindcasting and Forecasting and Coastal Hazards Symposium*, pp. 92–103. www.waveworkshop.org.

BADULIN, S. I., PUSHKAREV, A. N., RESIO, D. & ZAKHAROV, V. E. 2005 Self-similarity of wind-driven seas. *Nonlinear Process. Geophys.* **12**, 891–946.

BRETSCHNEIDER, C. L. 1952*a* The generation and decay of wind waves in deep water. *Trans. Am. Geophys. Union* **33**, 381–389.

BRETSCHNEIDER, C. L. 1952*b* Revised wave forecasting relationship. In *Proceedings of the 2nd Conference Coastal Engineering*, ASCE, Council on Wave Research.

BURLING, R. W. 1959 The spectrum of waves at short fetches. *Dtsch. Hydrogr. Z.* **12**, 96–117.

CARTER, D. J. T. 1982 Prediction of wave height and period for a constant wind velocity using the JONSWAP results. *Ocean Engng* **9** (1), 17–33.

CAULLIEZ, G. 2013 Dissipation regimes for short wind waves. *J. Geophys. Res. Oceans* **118**, 672–684.

CAULLIEZ, G., MAKIN, V. & KUDRYAVTSEV, V. 2008 Drag of the water surface at very short fetches: Observations and modeling. *J. Phys. Oceanogr.* **38**, 2038–2055.

DARBYSHIRE, J. 1959 Further investigation of wind generated waves. *Dtsch. Hydrogr. Z.* **12**, 1–13.

DELEONIBUS, P. S. & SIMPSON, L. S. 1972 Case study of duration-limited wave spectra observed at an open ocean tower. *J. Geophys. Res.* **77**, 4555–4569.

DOBSON, F., PERRIE, W. & TOULANY, B. 1989 On the deep water fetch laws for wind-generated surface gravity waves. *Atmos. Ocean* **27**, 210–236.

DONELAN, M. A. 1979 Marine forecasting. In *On the Fraction of Wind Momentum Retained by Waves*, pp. 141–159. Elsevier.

DUDIS, J. J. 1981 Interpretation of phase velocity measurements of wind-generated surface waves. *J. Fluid Mech.* **113**, 241–249.

GAGNAIRE-RENOU, E. 2009, Amélioration de la modélisation spectrale des états de mer par un calcul quasi-exact des interactions non-linéaires vague-vague. Thèse pour l'obtention du grade de docteur, Université du Sud Toulon Var, Ecole Doctorale Sciences Fondamentales et Appliquées.

GAGNAIRE-RENOU, E., BENOIT, M. & BADULIN, S. I. 2011 On weakly turbulent scaling of wind sea in simulations of fetch-limited growth. *J. Fluid Mech.* **669**, 178–213.

GARCIÁ-NAVA, H., OCAMPO-TORRES, F. J., OSUNA, P. & DONELAN, M. A. 2009 Wind stress in the presence of swell under moderate to strong wind conditions. *J. Geophys. Res.* **114**, C12008; doi:10.1029/2009JC005389.

GELCI, R., CAZALÉ, H. & VASSAL, J. 1957 Prévision de la houle. La méthode des densités spectroangulaires. *Bull. Comité Océanogr. Etude Côtes* **9**, 416–435.

GLAZMAN, R. 1994 Surface gravity waves at equilibrium with a steady wind. *J. Geophys. Res.* **99** (C3), 5249–5262.

HASSELMANN, K. 1962 On the nonlinear energy transfer in a gravity wave spectrum. Part 1. General theory. *J. Fluid Mech.* **12**, 481–500.

HASSELMANN, K. 1963*a* On the nonlinear energy transfer in a gravity wave spectrum. Part 2. Conservation theorems; wave-particle analogy; irreversibility. *J. Fluid Mech.* **15**, 273–281.

HASSELMANN, K. 1963*b* On the nonlinear energy transfer in a gravity wave spectrum. Evaluation of the energy flux and swell-sea interaction for a Neumann spectrum. Part 3. *J. Fluid Mech.* **15**, 385–398.

HASSELMANN, K. 1974 On the spectral dissipation of ocean waves due to white capping. *Boundary-Layer Meteorol.* **6**, 107–127.

HASSELMANN, K., BARNETT, T. P., BOUWS, E., CARLSON, H., CARTWRIGHT, D. E., ENKE, K., EWING, J. A., GIENAPP, H., HASSELMANN, D. E., KRUSEMAN, P., MEERBURG, A., MULLER, P., OLBERS, D. J., RICHTER, K., SELL, W. & WALDEN, H. 1973 Measurements of wind–wave growth and swell decay during the Joint North Sea Wave Project (JONSWAP). *Dtsch. Hydrogr. Z. Suppl.* **12**, (A8).

HASSELMANN, K., ROSS, D. B., MÜLLER, P. & SELL, W. 1976 A parametric wave prediction model. *J. Phys. Oceanogr.* **6**, 200–228.

HWANG, P. A. 2006 Duration- and fetch-limited growth functions of wind-generated waves parameterized with three different scaling wind velocities. *J. Geophys. Res.* **111**, C02005; doi:10.1029/2005JC003180.

HWANG, P. A., GARCIÁ-NAVA, H. & OCAMPO-TORRES, F. J. 2011 Observations of wind wave development in mixed seas and unsteady wind forcing. *J. Phys. Oceanogr.* **41** (12), 2343–2362.

HWANG, P. A. & SLETTEN, M. A. 2008 Energy dissipation of wind-generated waves and whitecap coverage. *J. Geophys. Res.* **113**, C02012. (2009 Corrigendum **113**, C02015; doi:10.1029/2008JC005244).

HWANG, P. A. & WANG, D. W. 2004 Field measurements of duration-limited growth of wind-generated ocean surface waves at young stage of development. *J. Phys. Oceanogr.* **34**, 2316–2326.

KAHMA, K. K. & CALKOEN, C. J. 1992 Reconciling discreapancies in the observed growth of wind-generated waves. *J. Phys. Oceanogr.* **22**, 1389–1405.

KAHMA, K. K. & CALKOEN, C. J. 1994 Growth curve observations. In *Dynamics and Modeling of Ocean Waves* (ed. G. J. Komen, L. Cavaleri, M. Donelan, K. Hasselmann, S. Hasselmann & P. A. E. M. Janssen), pp. 74–182. Cambridge University Press.

KATZ, A. V. & KONTOROVICH, V. M. 1971 Drift stationary solutions in the weak turbulence theory. *JETP Lett.* **14**, 265–267.

KATZ, A. V. & KONTOROVICH, V. M. 1974 Anisotropic turbulent distributions for waves with a non-decay dispersion law. *Sov. Phys. JETP* **38**, 102–107.

KATZ, A. V., KONTOROVICH, V. M., MOISEEV, S. S. & NOVIKOV, V. E. 1975 Power-like solutions of the kinetic Boltzmann equation for distributions of particles with spectral fluxes. *JETP Lett.* **21**, 5–6.

KAWAI, S. 1979 Generation of initial wavelets by instability of a coupled shear flow and their evolution to wind waves. *J. Fluid Mech.* **93**, 661–703.

KITAIGORODSKII, S. A. 1962 Applications of the theory of similarity to the analysis of wind-generated wave motion as a stochastic process. *Bull. Acad. Sci. USSR Ser. Geophys.* **N1**, 105–117; Engl. Transl.

KOMATSU, K. & MASUDA, A. 1996 A new scheme of nonlinear energy transfer among wind waves: RIAM method. Algorithm and perfomance. *J. Oceanogr. Soc. Japan* **52**, 509–537.

KOMEN, G. J., HASSELMANN, S. & HASSELMANN, K. 1984 On the existence of a fully developed wind-sea spectrum. *J. Phys. Oceanogr.* **14**, 1271–1285.

KOROTKEVICH, A. O., PUSHKAREV, A. N., RESIO, D. & ZAKHAROV, V. E. 2008 Numerical verification of the weak turbulent model for swell evolution. *Eur. J. Mech. (B/Fluids)* **27**, 361–387; doi:10.1016/j.euromechflu.2007.08.004.

LAVRENOV, I. V. 2003*a* A numerical study of a non-stationary solution of the Hasselmann equation. *J. Phys. Oceanogr.* **33** (3), 499–511.

LAVRENOV, I. V. 2003*b* *Wind Waves in Ocean. Physics and Numerical Simulation*. Springer.

LAVRENOV, I., RESIO, D. & ZAKHAROV, V. 2002 Numerical simulation of weak turbulent Kolmogorov spectrum in water surface waves. In *7th International Workshop on Wave Hindcasting and Forecasting*, pp. 104–116. Banff.

LIU, P. C. 1985 Testing parametric correlations for wind waves in the Great Lakes. *J. Great Lakes Res.* **11**, 478–491.

MERZI, N. & GRAF, W. H. 1985 Evaluation of the drag coefficient considering the effects of mobility of the roughness elements. *Ann. Geophys.* **3**, 473–478.

PIERSON, W. J. & MOSKOWITZ, L. A. 1964 A proposed spectral form for fully developed wind seas based on the similarity theory of S. A. Kitaigorodsii. *J. Geophys. Res.* **69**, 5181–5190.

PUSHKAREV, A. N., RESIO, D. & ZAKHAROV, V. E. 2003 Weak turbulent theory of the wind-generated gravity sea waves. *Phys. D: Nonlin. Phenom.* **184**, 29–63.

PUSHKAREV, A. & ZAKHAROV, V. On nonlinearity implications and wind forcing in Hasselmann equation, 2015, *Preprint*, arXiv:1212.6522v1 e-prints.

ROMERO, L. & MELVILLE, W. K. 2010 Airborne observations of fetch-limited waves in the Gulf of Tehuantepec. *J. Phys. Oceanogr.* **40**, 441–465.

SVERDRUP, H. V. & MUNK, W. H. Wind, sea, and swell: Theory of relations for forecasting, 1947, Hydrographic Office Pub. 60, US Navy.

TOBA, Y. 1961 Drop prediction by bursting of air bubbles on the sea surface (III). Study by use of a wind flume. *Mem. Coll. Sci., Univ. Kyoto. Ser. A* **29**, 313–344.

TOBA, Y. 1972 Local balance in the air–sea boundary processes. Part I. On the growth process of wind waves. *J. Oceanogr. Soc. Japan* **28**, 109–121.

TOBA, Y. 1973*a* Local balance in the air–sea boundary processes. II. Partition of wind stress to waves and current. *J. Oceanogr. Soc. Japan* **29**, 70–75.

TOBA, Y. 1973*b* Local balance in the air–sea boundary processes. III. On the spectrum of wind waves. *J. Oceanogr. Soc. Japan* **29**, 209–220.

TRACY, B. & RESIO, D. 1982 Theory and calculation of the nonlinear energy transfer between sea waves in deep water. *WES Rep. 11*. US Army, Engineer Waterways Experiment Station, Vicksburg, MS.

WEBB, D. J. 1978 Non-linear transfers between sea waves. *Deep-Sea Res.* **25**, 279–298.

WIEGEL, R. L. 1961 Wind waves and swell. In *Proc. 7th Conf. Coastal Eng.*, pp. 1–40. The Engineering Foundation, Council on Wave Research.

YEFIMOV, V. V. & BABANIN, A. V. 1991 Dispersion relation for the envelope of groups of wind waves. *Izv. Atmos. Ocean. Phys.* **27**, 599–603.

YOUNG, I. R. 1999 *Wind Generated Ocean Waves*. Elsevier.

YOUNG, I. R. & VAN VLEDDER, G. 1993 A review of the central role of nonlinear interactions in wind–wave evolution. *Phil. Trans. R. Soc. Lond.* **342**, 505–524.

ZAKHAROV, V. E. 1999 Statistical theory of gravity and capillary waves on the surface of a finite-depth fluid. *Eur. J. Mech. (B/Fluids)* **18**, 327–344.

ZAKHAROV, V. E. 2002 Theoretical interpretation of fetch limited wind-driven sea observations. In *7th International Workshop on Wave Hindcasting and Forecasting*, pp. 86–92.

ZAKHAROV, V. E. 2005 Theoretical interpretation of fetch limited wind-driven sea observations. *Nonlinear Process. Geophys.* **12**, 1011–1020.

ZAKHAROV, V. E. 2010 Energy balance in a wind-driven sea. *Phys. Scr.* T **142**, 014052.

ZAKHAROV, V. E. & BADULIN, S. I. 2011 On energy balance in wind-driven seas. *Dokl. Earth Sci.* **440** (Part 2), 1440–1444.

ZAKHAROV, V. E. & FILONENKO, N. N. 1966 Energy spectrum for stochastic oscillations of the surface of a fluid. *Sov. Phys. Dokl.* **160**, 1292–1295.

ZAKHAROV, V. E., LVOV, V. S. & FALKOVICH, G. 1992 *Kolmogorov Spectra of Turbulence. Part I.* Springer.

ZAKHAROV, V. E., RESIO, D. & PUSHKAREV, A. N. New wind input term consistent with experimental, theoretical and numerical considerations, 2012, *Preprint*, arXiv:1212.1069v1 e-prints.

ZAKHAROV, V. E. & ZASLAVSKY, M. M. 1983 Dependence of wave parameters on the wind velocity, duration of its action and fetch in the weak-turbulence theory of water waves. *Izv. Atmos. Ocean. Phys.* **19** (4), 300–306.

ZAVADSKY, A., LIBERZON, D. & SHEMER, L. 2013 Statistical analysis of the spatial evolution of the stationary wind wave field. *J. Phys. Oceanogr.* **43**, 65–79.